

THESIS FOR THE DEGREE OF DOCTOR OF PHILOSOPHY IN NATURAL SCIENCE,  
SPECIALIZATION IN CHEMISTRY

# Atmospheric Oxidation: Formation and Aging of Biogenic and Traffic-related Secondary Aerosols

Ågot Kirsten Watne



**UNIVERSITY OF GOTHENBURG**

Department of Chemistry and Molecular Biology  
University of Gothenburg  
SE-412 96 Gothenburg,  
Sweden

Doctoral thesis submitted for fulfilment of the requirements for the degree of  
Doctor of Philosophy in Chemistry

Atmospheric Oxidation: Formation and Aging of Biogenic and Traffic-related  
Secondary Aerosols

© Ågot Kirsten Watne, 2018

Atmospheric Science,  
Department of Chemistry and Molecular Biology,  
University of Gothenburg,  
SE-412 96 Gothenburg,  
Sweden

Printed by BrandFactory  
Källered, Sweden

ISBN 978-91-629-0386-2 (PRINT)

ISBN 978-91-629-0387-9 (PDF)

<http://hdl.handle.net/2077/54577>

## Abstract

---

Atmospheric aerosol particles affect the quality of life by influencing climate and by being a significant component of air pollution. Once a particle is released into or formed in the atmosphere, several processes begin to transform its physical and chemical properties. A considerable fraction of the particulate matter is secondary material i.e. formed from gas-to-particle conversion in the atmosphere. This secondary particle formation is an important process in the evolution of atmospheric aerosols. The aim of this thesis is to study the formation and aging of secondary aerosols by experimentally simulating atmospheric oxidation of emissions from biogenic and traffic-related sources. In this work the focus is on particle size, mass and number concentration, as well as on the thermal properties of the particles formed. These measures give insight into properties relevant for understanding the evolution of particles in the ambient atmosphere.

The thermal properties of secondary organic aerosols (SOA) formed from oxidation of monoterpenes in two oxidation flow reactors, G-FROST and PAM, and the atmospheric simulation chamber SAPHIR, was studied using a Volatility Tandem DMA (VTDMA). The detailed laboratory studies show that the formation of monoterpene SOA and its thermal properties depend on chemical structure of the precursor and oxidizing conditions. Furthermore, freshly formed monoterpene SOA comprise of compounds with a wide distribution of volatilities ranging from extremely low volatile to semi volatile compounds. Photochemical aging of SOA was studied in SAPHIR by oxidation induced by natural sun light and in PAM by exposing SOA precursors to high concentration of OH over a short time. The results reveal two opposing processes which drive the evolution of SOA volatility in the two systems.

During the course of this work an oxidation flow reactor, Go:PAM, has been developed. Go:PAM enables studies of secondary particle formation from rapidly changing emission sources, and was used to derive fuel-specific secondary particle emission factors from in-use transit buses under real-world driving conditions. Both primary emissions and the secondary particle formation of 29 buses running on conventional or on more sustainable fuels were investigated. The results emphasize the importance of taking the reduction in OH exposure into consideration when interpreting the secondary particle formation from plumes. However, independent of fuel and technology of the buses, the formation of secondary particulate mass was significantly higher than the primary particle mass. Furthermore, the results indicate there are emissions of non-fuel related compounds that are important for secondary particle formation.

This work provides insight in the formation and aging of secondary particles from biogenic and traffic-related sources. The results highlight the importance of including secondary particle formation when predicting the climate forcing of SOA and designing of air quality strategies.

**Keywords:** volatility, ozonolysis, hydroxyl radical, OH exposure,  $\alpha$ -pinene,  $\beta$ -pinene, limonene, dimer esters, engine exhaust, bus exhaust, air pollution, climate, oxidation flow reactor, atmospheric simulation chamber

## Abstrakt

---

Partiklar i atmosfären påverkar klimatet och utgör en väsentlig del av luftföroreningar. Dessa partiklar kan antingen släppas ut direkt från en källa eller bildas sekundärt i atmosfären. Atmosfäriska processer ändrar partiklarnas kemiska och fysiska egenskaper. Bildning av sekundär partikel massa är en viktig process för denna förändringen och vår förståelse av denna process är bristfällig. Syftet med arbetet som ligger till grund för denna avhandling var att studera bildning och åldring av sekundära partiklar och därmed bidra till ökad förståelse av de processer som påverkar egenskaperna på partiklarna. Detta gjordes genom att simulera bildning och åldring av sekundära partiklar från biogena ämnen och emissioner från trafik i flödesrör samt en stor så kallad simulerings kammare. Fokuset i arbetet har varit att studera ändringar i partikelstorlek, antal- och masskoncentration samt hur flyktiga partiklarna är. Flyktigheten är en viktig egenskap då den är avgörande för hur motståndskraftig partiklen är i atmosfären.

Bildning och åldring av biogena partiklar studerades i två typer av flödesrör, G-FROST och PAM, och i en simulerings kammare, SAPHIR, med hjälp av en Volailtiy Tandem DMA (VTDMA). Detaljerade laborations försök visade att den kemiska strukturen för ämnet som oxideras samt oxidationsförhållanden spelar en viktig roll för egenskaperna och mängden sekundär partikel massa som bildas. Vidare visar resultaten att när oxidationen startar och ny partikel massa bildas, så bildas både relativt flyktiga ämnen och ämnen som är så lågflyktiga att de kan bidra till bildning av nya partiklar. Jämförelse av hur sekundära biogena partiklar åldras i PAM och SAPHIR, belyser att det är två motsatta processer som driver åldringen av partiklarna i de två systemen. Detta är viktig kunskap för att förstå hur sekundära partiklar påverkar klimatet.

Sekundära partiklar spelar också en viktig roll för luftkvaliteten och i stadsmiljö är ofta utsläpp från trafik dominerande. Som en del av arbetet har en ny typ av flödesrör, som gör det möjligt att studera bildning av sekundär partikel massa från fordons plymer, utvecklats. Resultatet från tester på bussar visar att det var en signifikant ökning av sekundär partikelmassa oberoende av bränsle och teknik. Detta understryker betydelsen av att inkludera sekundär partikelbildning från trafik för att kunna vidta de mest effektiva åtgärder för luftkvaliteten.

**Nyckelord:** organisk aerosol, ozonolys, atmosfärisk åldring, monoterpener, trafik, luftföroreningar, klimat, flödesrör, atmosfäriska simuleringskammare, volatilitet

# List of publications

---

## Publications included in this thesis work

- I. Influence of Humidity, Temperature, and Radicals on the Formation and Thermal Properties of Secondary Organic Aerosol (SOA) from Ozonolysis of  $\beta$ -Pinene.**  
Emanuelsson, E. U., Watne, Å. K., Lutz, A., Ljungström, E., & Hallquist, M. (2013). The Journal of Physical Chemistry A, 117(40), 10346-10358. doi:10.1021/jp4010218
  
- II. Ozone and OH-induced oxidation of monoterpenes: Changes in the thermal properties of secondary organic aerosol (SOA).**  
Watne, Å. K., Westerlund, J., Hallquist, Å. M., Brune, W. H., & Hallquist, M. (2017). Journal of Aerosol Science, 114, 31-41. doi:10.1016/j.jaerosci.2017.08.011
  
- III. High-Molecular Weight Dimer Esters Are Major Products in Aerosols from  $\alpha$ -Pinene Ozonolysis and the Boreal Forest.**  
Kristensen, K., Watne, Å. K., Hammes, J., Lutz, A., Petäjä, T., Hallquist, M., . . . Glasius, M. (2016). Environmental Science & Technology Letters, 3(8), 280-285. doi:10.1021/acs.estlett.6b00152
  
- IV. Parameterization of thermal properties of aging secondary organic aerosol produced by photo-oxidation of selected terpene mixtures.**  
Emanuelsson, E. U., Mentel, T. F., Watne, A. K., Spindler, C., Bohn, B., Brauers, T., . . . Hallquist, M. (2014). Environ Sci Technol, 48(11), 6168-6176. https://doi:10.1021/es405412p
  
- V. Fresh and Oxidised Emissions from in-Use Transit Buses running on diesel, RME and CNG (2017)** Å. K Watne, M. Psychoudaki, E. Ljungström, M. Le Breton, M. Jerksjö, H. Fallgren, M. Hallquist, Å. M. Hallquist. Manuscript for EST

# Table of Contents

<b>Abstract</b> .....	ii
<b>Abstrakt</b> .....	iii
<b>List of publications</b> .....	iv
<b>List of Abbreviations</b> .....	vi
1. Setting the scene.....	1
2. Atmospheric aerosols and oxidation chemistry.....	2
2.1 Atmospheric aerosols .....	2
2.1.1 General atmospheric aerosols.....	2
2.1.2 Formation and aging of atmospheric particles .....	4
2.2 Atmospheric emissions of secondary aerosol precursors .....	7
2.2.1 Biogenic VOC emissions .....	7
2.2.2 Traffic-related emissions .....	7
2.3 Atmospheric oxidation .....	9
2.3.1 Two important oxidants: the OH radical and ozone.....	9
2.3.2 Oxidation of VOCs and radical chemistry .....	11
2.3.3 Ozonolysis of Monoterpenes.....	13
3. Studying Atmospheric Oxidation.....	16
3.1 Oxidation flow reactors and atmospheric simulation chambers.....	16
3.1.1 O <sub>3</sub> as primary oxidant: G-FROST .....	17
3.1.2 OH as primary oxidant: PAM and Go:PAM .....	18
3.1.3 Experimental set-up in the monoterpenes experiments .....	23
3.2 Atmospheric simulation chambers .....	24
3.2.1 SAPHIR.....	24
3.3 Fuel related emission factors.....	25
4. Aerosols characterization .....	26
4.1 Particle number concentration and particle size distributions .....	26
4.2 Thermal properties .....	27
4.3 Particle chemical composition.....	30
4.4 Supporting measurements .....	30
5. Results and discussion.....	31
5.1 Oxidation of biogenic emissions .....	31
5.1.1 Radical chemistry and water concentration.....	31
5.1.2 Formation of dimer esters.....	34
5.1.3 Thermal properties of freshly formed SOA.....	35
5.2 Aging of Secondary Organic Aerosols.....	38
5.2.1 Oxidative aging in OFRs and chambers.....	38
5.3 Production of secondary aerosol mass from exhaust emissions .....	40
5.3.1 Studying exhaust emissions with Go:PAM.....	40
5.3.2 Secondary particle formation of emissions from in-use transit buses .....	41
6. Atmospheric implications.....	44
Acknowledgements .....	46
References .....	47

## List of Abbreviations

---

AVOC – Anthropogenic Volatile Organic Compounds  
BVOC – Biogenic Volatile Organic Compounds  
CI –Criegee Intermediate  
CNG – Compressed Natural Gas  
CPC – Condensation Particle Counter  
DMA – Differential Mobility Analyser  
DSL – Diesel  
EEPS – Engine Exhaust Particle Sizer  
EF – Emission factor  
ELVOC – Extremely Low Volatile Organic Compounds  
G-FROST – Göteborg Flow Reactor for Oxidation Studies at low Temperature  
Go:PAM – Göteborg Potential Aerosol Mass Reactor  
LVOC – Low Volatile Organic Compounds  
OFR – Oxidation Flow Reactor  
PAM – Potential Aerosol Mass Reactor  
PM – Particulate matter  
PN – Particle number  
POZ – Primary Ozonide  
RME – Rapeseed Methyl Ester  
SCI – Stabilised Criegee Intermediate  
SMPS – Scanning Mobility Particle Sizer  
SOA – Secondary Organic Aerosols  
SOZ – Secondary Ozonide  
SVOC – Semi Volatile Organic Compounds  
VFR- Volume Fraction Remaining  
VOC – Volatile Organic Compounds  
VTDMA – Volatility Tandem DMA





# 1. Setting the scene

The composition of the atmosphere has changed compared to pre-industrial times, and that affects the quality of life in many aspects. Daily we hear about the effects of global warming; intensified tropical storms, draughts and extreme heat waves. The climate is changing [Stocker et al., 2013]. The changed composition of the atmosphere also directly affects human health. We read alarming reports on bad air quality. Annually ambient air pollution cause 4.2 million premature deaths and atmospheric particles are a major cause [Cohen et al., 2017].

Atmospheric particles, i.e. nano sized particles, are important for climate [Stocker et al., 2013] and human health [Shiraiwa et al., 2017]. The particles can either be emitted directly to the atmosphere, i.e. primary particles, or be formed through gas to particle conversion, i.e. secondary particles. On a global scale, biogenic emissions of precursors for formation of secondary organic aerosols (SOA) are dominating [Hallquist et al., 2009]. The formation of secondary organic particles from atmospheric oxidation of gaseous compounds is complex, and the understanding of this process is still incomplete [Hallquist et al., 2009]. Therefore, when the climate forcing of SOA is predicted, this complexity needs to be reduced, and thus predictions of this forcing are less accurate [Shrivastava et al., 2017]. On a local and regional scale, traffic-related emissions can be a major source of secondary aerosols precursors [Dunmore et al., 2015; Ots et al., 2016], and consequently the choice of fuel and technology of the vehicles will have an impact on the air quality. In order to meet the challenges with increased energy demand and the need to reduce greenhouse gas emissions in connection with transportation, there is a call to change from conventional fuels to more sustainable fuels. However, the effect this change has on air quality is generally not well understood.

In order to take appropriate actions to maintain high quality of life for as many as possible, we need to understand the consequences of a changed composition of the atmosphere. Knowledge of the formation and evolution of secondary aerosols is needed to predict societal challenges related to climate change and human health impacts. In turn, natural and societal responses will have feedback on the same processes. The objective of this thesis is to contribute to this understanding.

## **2. Atmospheric aerosols and oxidation chemistry**

A major part of this thesis deals with formation and aging of secondary aerosols and some basic principles of atmospheric oxidation chemistry are introduced in this chapter. In addition, some fundamental concepts describing atmospheric aerosols and their evolution, as well as a brief description of biogenic and traffic-related emissions are provided here.

### **2.1 Atmospheric aerosols**

Atmospheric aerosol particles have natural and anthropogenic sources, and consist of both organic and inorganic compounds. Windblown dust, sea spray, volcanic particles and bio aerosols are examples of naturally produced primary particles, while particles emitted from traffic, biomass burning and industry are examples of particles from anthropogenic sources. However, the division of atmospheric aerosol particles into primary and secondary is generally too simple due to a dynamic exchange between the gas and particulate phase as the aerosol is aged in the atmosphere [Donahue et al., 2012; Jimenez et al., 2009].

#### **2.1.1 General atmospheric aerosols**

Atmospheric aerosols are a heterogeneous and dynamic mix of particles and gases. As can be seen from Figure 2.1, atmospheric aerosol particles span over a wide size range, from a few nanometers to up to about 100  $\mu\text{m}$ . In order to be defined as an aerosol particle, the particle has to be stable in the suspended gas for at least a few seconds. Atmospheric aerosols are often polydisperse, i.e. contain particles of a wide size range, but in laboratory studies monodisperse aerosols, i.e. contains particles of the same size, are often used.

The chemical composition of atmospheric aerosol particle depends strongly on the emission source and in which environment the aerosol is aged. In atmospheric particles there is often a large fraction of organics [Kanakidou et al., 2005], and a significant portion has a secondary origin, i.e. SOA [Jimenez et al., 2009]. In addition to organics, aerosol particles are in general composed of inorganics such as sulfate, nitrate, ammonium, chloride and trace metals that may also influence the chemistry and affects health and climate. The complexity of aerosol particles is thus a major challenge, and in relation to other gaseous air pollutants there is still a lot more to understand in order to accurately predict particle effects on climate and health.

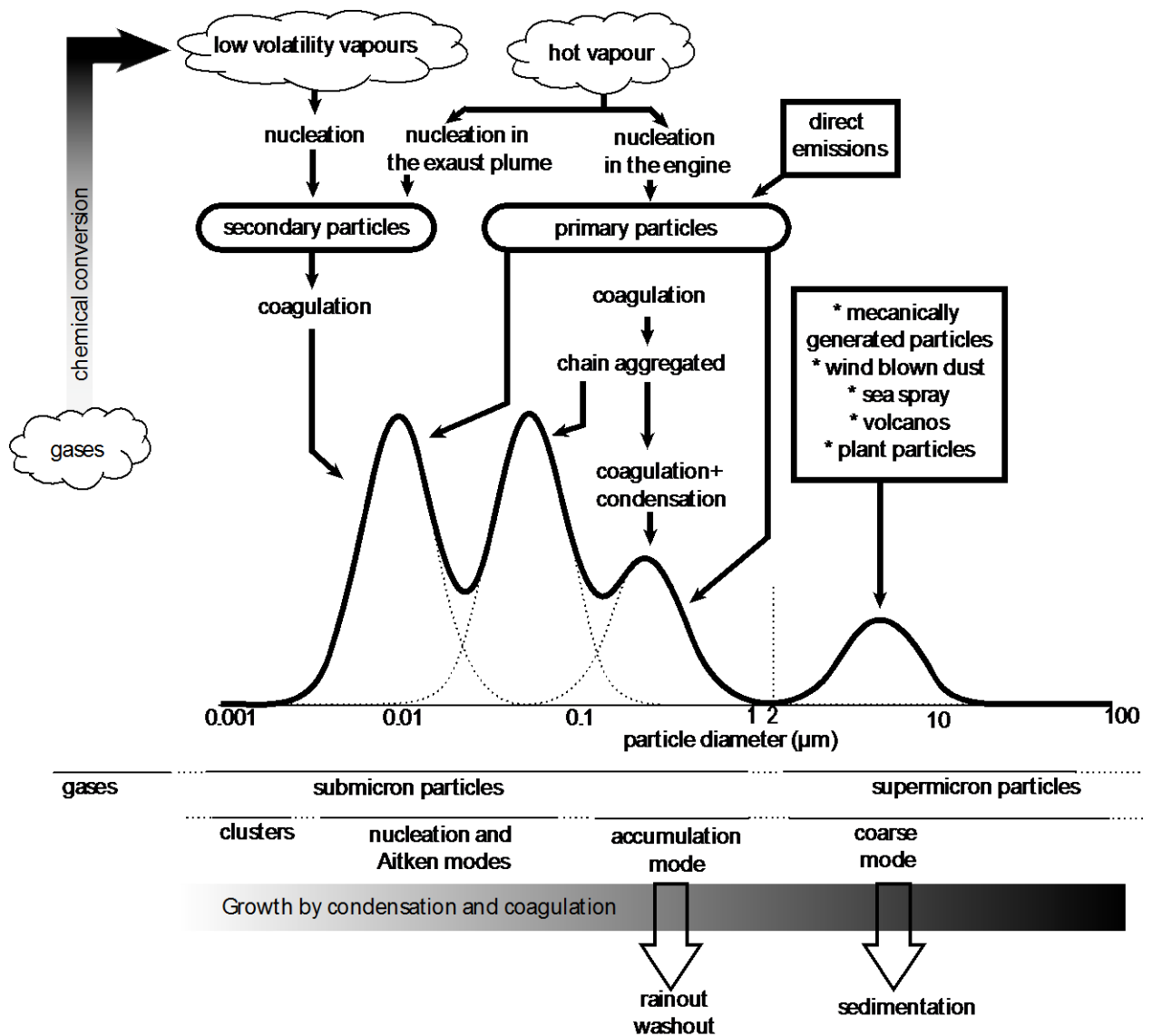


**Figure 2.1** Overview of aerosol size classification together with main sources and sinks. Graphic design by Eva Emanuelsson. Printed with permission.

Atmospheric particles influence the climate and human health. The Earth radiative budget is directly affected by particles either absorbing or scattering light, and indirectly by playing an important role in atmospheric chemistry and in cloud formation. Although it is quite well agreed upon that atmospheric particles affect the climate, there are still large gaps in our understanding of the effects [Stocker et al., 2013]. There are particular uncertainties in the formation and properties of the secondary aerosols [Hallquist et al., 2009; Shrivastava et al., 2017]. Epidemiological studies have uncovered clear relationships of particulate matter with cardiovascular and respiratory diseases [Shiraiwa et al., 2017], and recent findings indicate that there is a link between inhaled particles and brain damage [Maher et al., 2016]. Most legislation concerning particulate matters is given for PM<sub>2.5</sub>, i.e. the concentration of particles with a diameter of less than 2.5 µm. However, it is unclear if this is the best measure for the health effects of particle exposure [Cassee et al., 2013; Shiraiwa et al., 2017].

## 2.1.2 Formation and aging of atmospheric particles

In the atmosphere, due to attractive forces between molecules, clusters are continuously formed. Most of the clusters are unstable and will fall apart; however, if the cluster reaches a certain size, the Kelvin diameter, a stable particle can be formed. In order for gas phase compounds to contribute to this new particle formation, the vapor pressure needs to be sufficiently low, but as the new particle has formed, compounds with higher vapor pressure can contribute to condensational growth. The evolution of the organic aerosol particle is primarily driven by partitioning of molecules between the gas phase and the condensed phase and condensed phase reactions.

The equilibrium distribution between gas and condensed phase is given by Raoult's law. A more practical form for atmospheric purposes, based on Raoult's law is to use a partitioning coefficient ( $\kappa_i$ ), defined by the adsorptive gas partitioning theory given by Equation 2.1 [Pankow, 1994].

$$K_i = \frac{c_i^{cond}}{c_i^{vap} M_{org}} = \frac{RT f_{org}}{MW_{org} \gamma_i p_{i0}} \quad (\text{Eq 2.1})$$

where  $M_{org}$  is the total suspended particulate matter,  $c_i^{cond}$  and  $c_i^{vap}$  are the mass concentrations in the condensed phase and gas phase, respectively,  $p_{i0}$  is the saturation vapor pressure,  $\gamma_i$  is the activity coefficient,  $MW_{org}$  is the average molecular weight of all organic molecules in the particle,  $f_{org}$  is the weight fraction of organic matter,  $R$  is the gas constant and  $T$  is the temperature. As can be seen from Equation 2.1, the distribution of a compound between gas and condensed phase does not only depend on its molecular properties and temperature, but also on the total concentration of particulate matter. This implies that by diluting of the aerosol, i.e. reducing the concentration of total suspended particulate matter, the chemical composition of the particle will change due to evaporation of compounds from the condensed phase.

One of the key properties defining the distribution of a substance between condensed and gas phase is the saturation vapor pressure ( $p_i^0$ ). This is the pressure needed to maintain equilibrium with the gas phase over a flat surface of the pure substance. Atmospheric aerosols are rarely ideal systems; the gas- and condensed phase contain a mixture of compounds that can offset the activity coefficients from the ideal value of 1. Furthermore, atmospheric aerosol particles are often so small that the assumption of a plane surface will not hold, and the Kelvin effect is needed to be taken into account. To describe the vapor pressure of a compound  $i$  over a multicomponent system, the equilibrium vapor pressure is given by Equation 2.2:

$$p_i(D_p) = \gamma_i \chi p_i^0 \exp\left(\frac{4\sigma v_{m,i}}{RT D_p}\right) \quad (\text{Eq 2.2})$$

where  $\gamma_i$  is the activity coefficient,  $\chi$  is the mole fraction of  $i$  in the mixture,  $\sigma$  is the surface tension,  $v_{m,i}$  the molar volume of  $i$  in the mixture,  $R$  is the common gas constant,  $T$  is temperature and  $D_p$  is the diameter of the particle. The activity coefficient accounts for the deviation from ideal behavior. From Equation 2.2 it can be seen that for smaller particle sizes a vapor pressure higher than the saturation vapor pressure is needed to maintain the mass equilibrium.

The concept of volatility provides a framework which allows simplifying the description of atmospheric aerosols. The volatility is no single chemical or physical property, but rather is a combination of the saturation vapor pressure, phase state, the size of the particle as well as the mixing and reactions of compounds in the particle phase. In the atmosphere, a particle containing partly volatile components may partly evaporate and lose these components. In doing so, size, molar ratio and activity coefficients may change and less volatile components will start to dominate and make the remains more persistent. In atmospheric studies, the volatility is usually described by the saturation mass concentration ( $C^*$ ) which is the mass concentration of a compound needed to maintain the mass equilibrium between the gas and condensed phase, often given in the units of  $\mu\text{g}/\text{m}^3$ . Based on this, atmospheric organic compounds are often described on the basis by their saturation mass concentration, and often in the terms of intermediate volatile VOCs (IVOC), semi volatile VOCs (SVOC), low volatile VOCs (LVOC) and extremely low volatile VOCs (ELVOC) [Donahue et al., 2011]. SVOC and LVOC can be present both in the particle and gas phase, while ELVOC for most cases will only be found in the particle phase [Donahue et al., 2011; Ehn et al., 2014]. However, it should be noted that in the literature these terms and definitions not always strictly used by the definition outlined by Donahue et al (2006, 2011). For example, in this work SVOC and ELVOC are defined on the basis of data from the measurements using a volatility DMA (VTDMA).

The phase state of the particle is affecting the reactivity as well as the evaporation rate. Studies indicates that SOA particles have a high viscosity which implies that it may not be correct to assume that SOA particles are liquid [Cappa and Wilson, 2011; Vaden et al., 2011; Virtanen et al., 2010]. A more viscous particle will evaporate more slowly compared to a liquid particle. Furthermore, chemical reaction within the particle is slowed down as the viscosity is increasing. Generally, condensed phase reactions produce compounds with lower vapor pressure, and so reduce the general volatility of the particle [Shrivastava et al., 2015]. However, it should be noted that for these reactions to be important, the reaction time need to be shorter than the life-time of the compound due to evaporation.

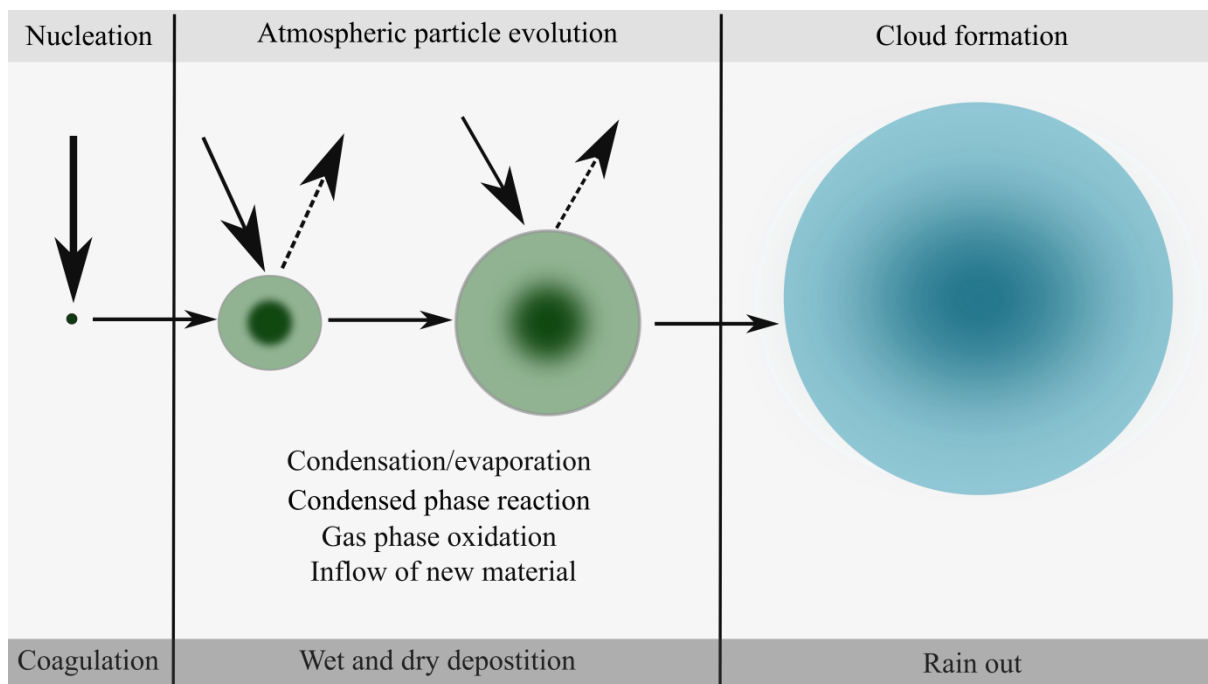


**Figure 2.2** *Evolution of atmospheric particles.*

Atmospheric particle evolution is illustrated in Figure 2.2. As new particles are formed through nucleation of extremely low volatility compounds, the particles will grow by condensation and undergo chemical and physical changes including partial evaporation. All these processes will alter the chemical and physical properties of the particle. When the size of the particle reaches that of cloud condensation nuclei, the particle can become a cloud droplet. As indicated in Figure 2.2, not all particles formed through nucleation will reach the size of cloud condensation nuclei or have a suitable composition. Small particles can be removed by coagulation and larger particles can be removed by wet and dry deposition [Shrivastava et al., 2015; Vehkamäki and Riipinen, 2012].

## 2.2 Atmospheric emissions of secondary aerosol precursors

Biogenic and anthropogenic sources emit gases and particles to the atmosphere. One important and heterogeneous group of gases is VOCs which play a significant role for the formation of secondary organic aerosols (SOA) [Glasius and Goldstein, 2016], and is emitted from both sources. In addition, traffic emits inorganic compounds, which can interact and contribute to the formation of secondary aerosols.

### 2.2.1 Biogenic VOC emissions

Biogenic VOCs produced by plants are involved in plant growth, development, reproduction and defense [Laothawornkitkul et al., 2009]. Globally, vegetation emits about 1000 Tg BVOCs every year, whereof 50 % is isoprene, 15 % monoterpenes and 3% sesquiterpenes [Guenther et al., 2012]. Monoterpenes and sesquiterpenes are of special interest since the atmospheric oxidations of these compounds efficiently produce SOA [Palm et al., 2016]. In this thesis the focus has been on SOA formation from oxidation of three important monoterpenes:  $\alpha$ -pinene,  $\beta$ -pinene and limonene. The atmospheric emissions of monoterpenes have a seasonal variation, with a maximum during summer [Hakola et al., 2012; Hakola et al., 2009; Seco et al., 2011]. In the boreal forest, the concentration of  $\alpha$ -pinene is significant from early spring to late autumn, whereas the concentrations of  $\beta$ -pinene and limonene are only significant in summer and early autumn [Hakola et al., 2012].

### 2.2.2 Traffic-related emissions

Traffic-related sources contribute to the air pollution by both exhaust emissions and production of non-combustion particles, e.g. particles produced from breaks, tires and road surface wear [Grigoratos and Martini, 2014]. In this thesis the focus has been on exhaust emissions. Generally, engine exhaust consists primarily of nitrogen, oxygen, water vapor and CO<sub>2</sub>, with minor constituents of CO, hydrocarbons and NO<sub>x</sub> [Matti Maricq, 2007]. In addition, particulate matter is emitted, including soot, organic material and trace metals [Dallmann et al., 2014; Lough et al., 2005]. Figure 2.3 illustrates the evolution of vehicle exhaust as it is emitted into the ambient air. The exhaust is hot when emitted, but cools quickly as it is diluted with ambient air, and the cooling promotes nucleation and condensation of exhaust compounds on existing particles, i.e. formation of secondary particles. However, as the exhaust is diluted, the gas phase concentration of pollutants is reduced, leading to evaporation of compounds from the particles in order to maintain phase equilibrium. Furthermore, some of the emitted gaseous compounds can react in the atmosphere and be transformed to compounds of lower

volatility, contributing to chemically induced particle formation. The formation of chemically induced secondary particulate matter often exceeds the emissions of primary particulate matter [Alanen et al., 2017; Gordon et al., 2014a; Gordon et al., 2014b; Karjalainen et al., 2016a; Platt et al., 2013; Tkacik et al., 2014].

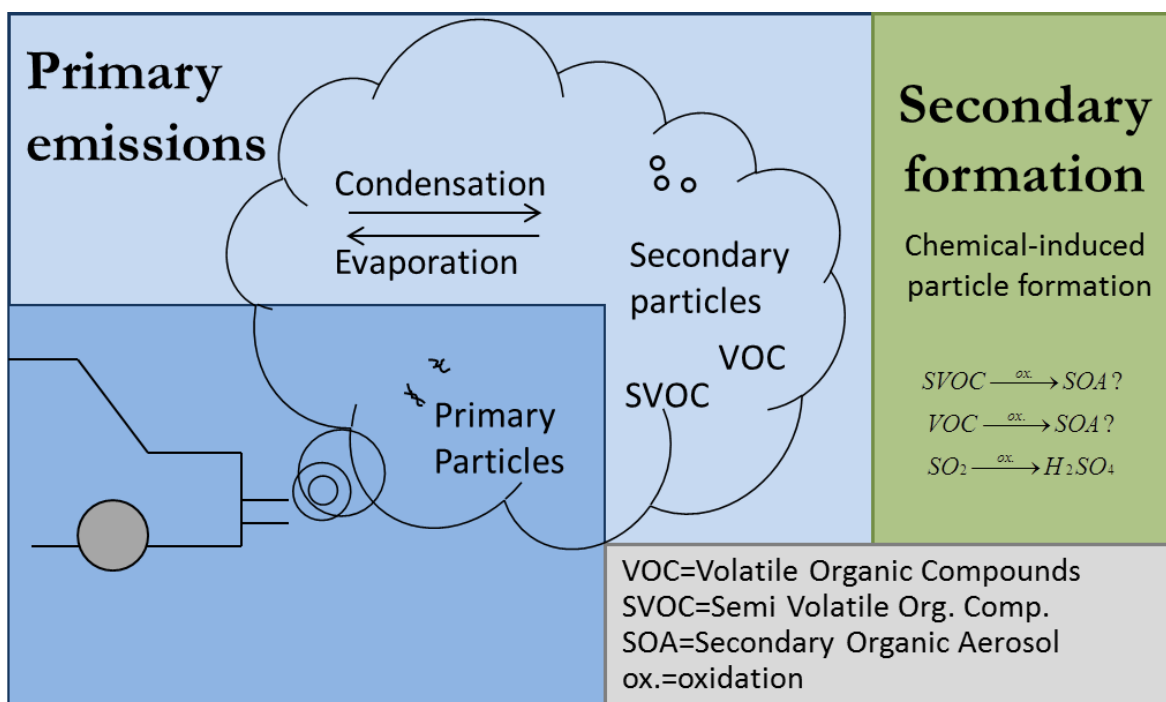


**Figure 2.3** Evolution of exhaust emissions. Graphic design by Åsa Hallquist. Printed with permission.

While there are considerable differences in the primary particle emissions from vehicles depending e.g. on fuel, technology and exhaust after treatment [Hallquist et al., 2013; Pirjola et al., 2016; Pourkhesalian et al., 2014], the variation is less pronounced for the secondary particle formation [Friedman et al., 2017; Jathar et al., 2017]. There are, however, still many open questions considering the formation of secondary aerosols from vehicle emissions [Gentner et al., 2017], and the increased primary emissions during real-world traffic compared to laboratory tests [Pirjola et al., 2017] calls for studying the formation of secondary aerosol formation under real-world driving conditions.



## 2.3 Atmospheric oxidation

The atmosphere is a large chemical reactor with a myriad of chemical compounds that can react in innumerable ways under changing physical conditions, with the sun turning on and off the photochemistry. It is clear from thermodynamics that the final products of carbon-, hydrogen-, nitrogen- and sulfur-containing gases in air are carbon dioxide, water, nitrate and sulfate, respectively. The path to these products is often long and complicated but it normally starts with an attack by an oxidizing agent i.e. hydroxyl radical (OH), ozone (O<sub>3</sub>) or nitrate radical (NO<sub>3</sub>). The relative importance of the oxidants depends on the oxidant concentrations and the molecular structure of the precursor as well as humidity, radical conditions and temperature. In this work atmospheric oxidation by OH and O<sub>3</sub> has been studied.

### 2.3.1 Two important oxidants: the OH radical and ozone

OH is the most important oxidation agent during daytime, but O<sub>3</sub> is an important oxidant due to high concentrations and the special case with oxidation of alkenes. Furthermore, O<sub>3</sub> is present both daytime and nighttime. As can be seen from Table 2.1, the OH initiated oxidation is faster and less specific than oxidation by O<sub>3</sub>.

**Table 2.1:** Atmospheric life time for  $\alpha$ -pinene,  $\beta$ -pinene and limonene for their reaction with O<sub>3</sub> and OH

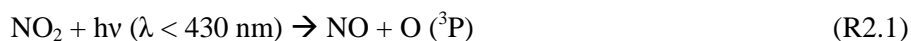
VOC	Lifetime (h) for reaction with	
	OH <sup>a</sup>	O <sub>3</sub> <sup>b</sup>
$\alpha$ -pinene	5,3 <sup>c</sup>	4,0 <sup>d</sup>
$\beta$ -pinene	3,7 <sup>c</sup>	17,9 <sup>e</sup>
Limonene	1,7 <sup>c</sup>	1,3 <sup>e</sup>

<sup>a</sup>Assumed a OH concentration of  $1 \times 10^6$  molecules cm<sup>-3</sup> [Finlayson-Pitts and Pitts Jr, 2000].

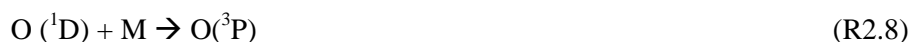
<sup>b</sup>Assumed a O<sub>3</sub> concentration of  $7 \times 10^{11}$  molecules cm<sup>-3</sup> [Atkinson and Arey, 2003]

Rate constants from [Atkinson and Arey, 2003]<sup>c</sup>, [Stewart et al., 2013]<sup>d</sup>, [Khamaganov and Hites, 2001]<sup>e</sup>

In the troposphere, ozone is primarily produced through the photolysis of NO<sub>2</sub> (R2.1-2.2), and the background concentrations in a clean atmosphere is normally around 7×10<sup>11</sup> molecules cm<sup>-3</sup> [Atkinson and Arey, 2003]. In a polluted atmosphere with elevated concentrations of NO<sub>2</sub> and organics, the concentration of ozone will be higher due the reaction of NO with hydro peroxy radicals and alkyl peroxy radicals (R2.4 and R2.5).



The atmospheric OH concentration is only controlled by in situ chemistry due to its high reactivity. The main source of OH in the atmosphere is from photolysis of O<sub>3</sub> with subsequent reaction of O(<sup>1</sup>D) with water (R2.6-2.7).



In addition, OH can e.g. be formed from photolysis of HONO and H<sub>2</sub>O<sub>2</sub> and from the ozone induced oxidation of alkenes. During day time a significant fraction of the OH radicals can be produced from the ozonolysis of alkenes, and during night time this reaction is the domination source of OH [Vereecken and Francisco, 2012]. Given the right conditions, daytime OH concentrations of 2×10<sup>7</sup> molecules cm<sup>-3</sup> can be reached [Stone et al., 2012]. However, normally it ranges in polluted environments from 1.2 to 6×10<sup>6</sup> molecules cm<sup>-3</sup> and in environments influenced by biogenic emissions from 2 to 15 ×10<sup>6</sup> molecules cm<sup>-3</sup> [Stone et al., 2012].

### 2.3.2 Oxidation of VOCs and radical chemistry

Oxidation of VOCs is a key feature in atmospheric chemistry, and as illustrated in Figure 2.4, the fate of VOCs is a competition between fragmentation to complete oxidation to CO<sub>2</sub> and water, and formation of products with lower vapor pressure [Goldstein and Galbally, 2007]. Simplified, the vapor pressure will decrease by increasing the number of carbons or increased functionality, i.e. addition of functional groups. VOCs will also be removed from the atmosphere through wet and dry deposition [Shrivastava et al., 2015].

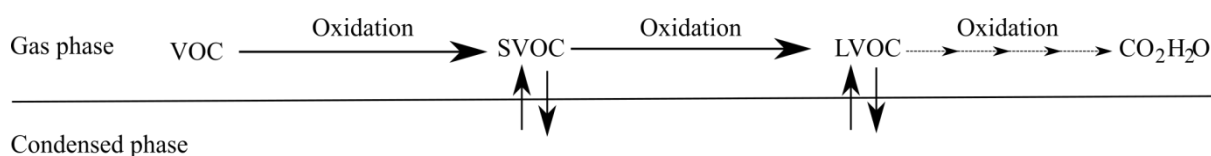


**Figure 2.4** Schematic of multigenerational gas phase oxidation and partitioning to condensed phase. Note that surface and condensed phase processes are not shown.

As an example of atmospheric oxidation a schematic of OH radical induced oxidation is shown in Figure 2.5. Depending on the structure of the parent VOC, OH will either abstract an H and form water or be added to the parent VOC, and in both cases an alkyl radical (R) is formed. Alkyl radicals can also be formed from decomposition of reactive species. In the atmosphere nearly all alkyl radicals react with molecular oxygen (O<sub>2</sub>) to form an alkyl peroxy radical (RO<sub>2</sub>). In a polluted atmosphere, the fate of RO<sub>2</sub> will mainly be the reaction with NO forming an alkoxy radical (RO). RO<sub>2</sub> radicals can also react with NO<sub>2</sub> forming peroxy nitrates, i.e. PAN like compounds. These compounds are important because they are relatively stable, and therefore can transport NO<sub>x</sub> to pristine environments.

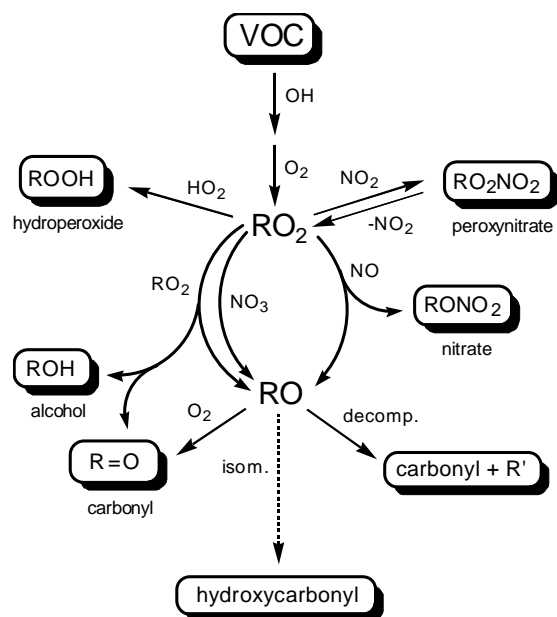


**Figure 2.5** Sequence of OH initiated VOC oxidation [Hallquist et al., 2009]. Printed with permission.

In absence of NO<sub>x</sub>, the self-reaction of alkyl peroxy radicals (RO<sub>2</sub> + RO<sub>2</sub>) and the reaction of alkyl peroxy radicals with hydro peroxy radicals (HO<sub>2</sub>) becomes more important [Vereecken and Francisco, 2012]. Of several possible reaction channels for the self-reaction, two channels are dominating: (i) the formation of two alkoxy radicals (RO) and molecular oxygen, and (ii) the formation of an alcohol, a carbonyl and molecular oxygen [Vereecken and Francisco, 2012]. For most alkyl peroxy radicals, the reaction channel with HO<sub>2</sub> forming a carboxylic acid and molecular oxygen is the most important, but there are also other reaction channels available [Orlando and Tyndall, 2012]. It should be noted that the reaction channels discussed above often due to high concentrations of RO<sub>2</sub> and HO<sub>2</sub> becomes important in laboratory studies. As can be seen from Figure 2.5, the alkoxy radical (RO) can (i) react with O<sub>2</sub> forming a carbonyl, (ii) isomerize or (iii) decompose forming a carbonyl and an alkyl radical (R). The formation of an alkyl radical starts the radical chain reaction all over again.

The basic atmospheric relevant radical reaction pathways are well-established [Orlando and Tyndall, 2012], but as the measurement techniques has become more sophisticated, new reaction pathways has been elucidated. Recently, formation of highly oxidized organic compounds in the gas phase has been observed, and it is believed that these compounds are formed from autoxidation of RO<sub>2</sub> radicals [Berndt et al., 2016; Ehn et al., 2014; Jokinen et al., 2015]. Autoxidation is the oxidation of a hydrocarbon by addition of molecular oxygen followed by intramolecular H-shifts, which can lead to a rapid production of extremely low volatility compounds. Studies indicate that the chemical structures of monoterpenes are of importance for the formation of these extremely low volatile compounds [Ehn et al., 2014; Jokinen et al., 2015].

### 2.3.3 Ozonolysis of Monoterpenes

As already mentioned, ozone induced oxidation of monoterpenes is important in atmospheric oxidation for several reasons. First, compounds formed in the ozonolysis of monoterpenes can contribute to formation of secondary organic aerosols. Second, formation of non-photolytic HO<sub>x</sub> radicals from the ozonolysis can contribute significantly to the atmospheric radical chemistry.

All monoterpenes have the same chemical formula, C<sub>10</sub>H<sub>16</sub>, but the chemical structure varies. The number and placement of double bonds determine the atmospheric oxidation chemistry of the monoterpenes. It is therefore important to distinguish between endocyclic monoterpenes, *i.e.* double bond within the ring, and exocyclic monoterpenes, *i.e.* double bond outside the ring. As can be seen from Figure 2.6,  $\alpha$ -pinene,  $\beta$ -pinene and limonene all have different placement of double bonds, and this structural difference makes the oxidation of these three monoterpenes interesting to study and compare.

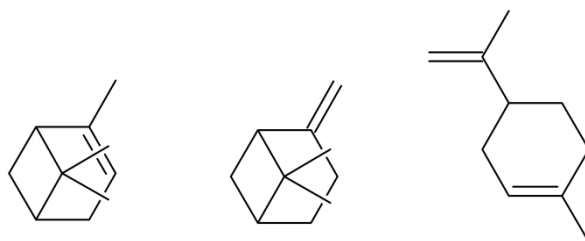


**Figure 2.6** Chemical structures of  $\alpha$ -pinene,  $\beta$ -pinene and limonene

Independent on the placement of the double bond, the ozonolysis of monoterpenes starts with an addition of ozone to the double bond. This will lead to formation of a primary ozononide (POZ) which is thermally unstable and rapidly will decompose. The initial cleavage of the carbon bond is a key feature for the further chemistry, and here the placement of the double bond plays an important role. For exocyclic and acyclic alkenes the cleavage will lead to formation of two fragments whereas the carbon cleavage for endocyclic alkenes will lead to a ring opening with the carbon chain kept intact. Illustrated for  $\beta$ -pinene in Figure 2.7, the decomposition of the primary ozononide will lead to formation of two alternative pairs of carbonyl oxides, *i.e.* Criegee Intermediates (CI) and carbonyls. While for endocyclic monoterpenes, the carbonyl functional group will be retained in the CI (Figure 2.8). However, in both cases the CI will be excited, and the fate of the excited CI will be a competition between unimolecular reactions and collisional stabilization to form a stabilized CI.

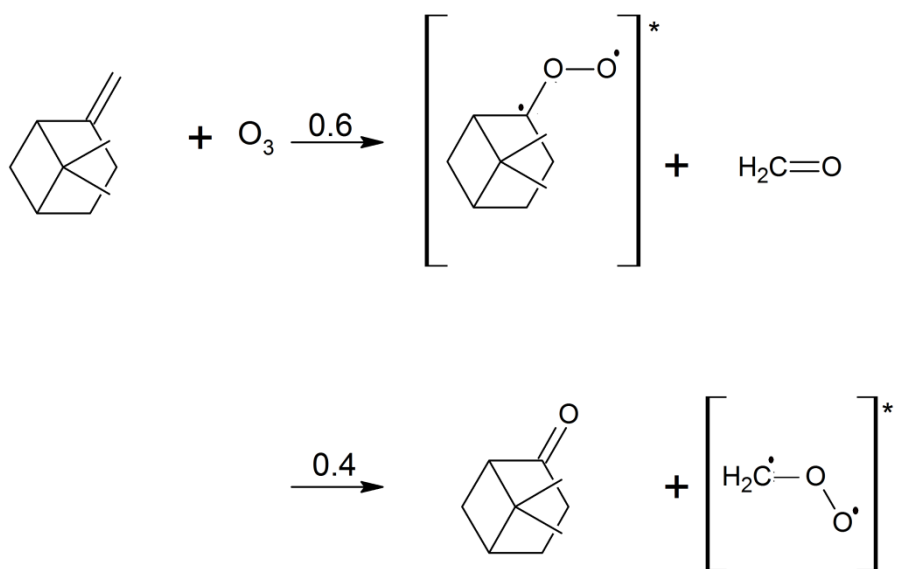


**Figure 2.7** Initial reaction steps in the ozonolysis of  $\beta$ -pinene

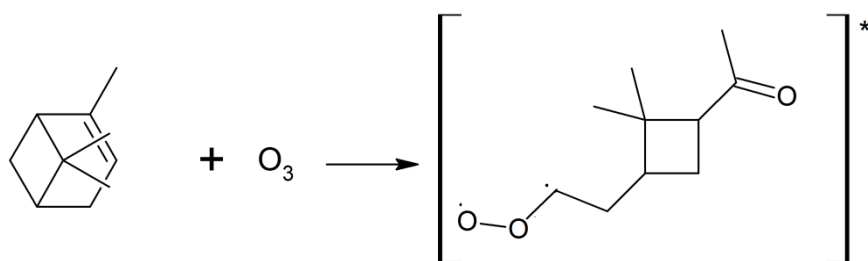


**Figure 2.8** Initial reaction steps in the ozonolysis of  $\alpha$ -pinene

The isomerization of the excited CI for small alkenes (e.g. monoterpenes) proceeds mainly through two channels [Vereecken and Francisco, 2012]. In the first channel, H-shift can occur if a suitable H-atom is available, and a vinylhydroperoxid radical is formed. This radical can fall apart forming a vinoxy radical and a hydroxyl radical (OH). In the second channel, the CI can isomerize through cyclisation, forming a dioxirane. The dioxirane can decompose by breaking the O-O bond and depending on the chemical structure of the parent VOC, rearrange to an acid or an ester. In addition to the unimolecular reactions of the excited CI, the excited CI can also become stabilized through collisions. The rate of stabilization depends strongly on the initial cleave of the carbon bond in the primary ozonide. Under ambient conditions, 40 % of the excited CI formed from the ozonolysis of  $\beta$ -pinene will be stabilized [Nguyen et al., 2009] whereas less than 15 % of the excited  $\alpha$ -pinene CI is stabilized [Vereecken and Francisco, 2012]. Stabilized CIs is suggested to in the gas phase react with e.g. water and oxygenated organic molecules forming secondary ozonides, carboxylic acids and dimer esters [Kristensen et al., 2014; Kristensen et al., 2013; Vereecken et al., 2012; Zhang et al., 2017].

In summary, the number and placement of double bonds determine to large extent which products that can be formed in the ozonolysis of monoterpenes. Furthermore, ambient conditions like humidity and temperature influence which reaction channels that are favored, and by that also influence the product distribution. It is therefore of great interest to do detailed studies of monoterpene oxidation in order to be able to describe the SOA formation.

### 3. Studying Atmospheric Oxidation

The complexity of atmospheric oxidation makes laboratory studies a necessary link between the ambient atmosphere and models. A variety of laboratory tools can be used to simulate atmospheric chemistry and aging, including oxidation flow reactors (OFRs) and atmospheric simulation chambers. The great benefit by using such devices is the possibility to isolate the processes of interest in a controlled reality. A tool used to employ results from atmospheric studies is emissions factors, and a brief description of the fuel-related emission factors is given in Section 3.5.

#### 3.1 Oxidation flow reactors and atmospheric simulation chambers

Both atmospheric simulation chambers and OFRs can be used to study atmospheric relevant oxidation and aging, however there are important differences between the two systems (cf Table 3.1). Generally, atmospheric simulation chamber are static which enables longer residence times and allows slower processes to take place (e.g. condensed phase processes). OFRs are dynamic systems with short residence time which facilitates systematic studies of varying reaction conditions (e.g. water concentration, radical chemistry and temperature). Furthermore, in OFRs high OH concentration can be achieved which enables studies with high OH exposures. The three oxidation flow reactors and the atmospheric simulation chamber used in this work are presented in Table 3.1.

*Table 3.1 Comparison of Oxidation flow reactors and atmospheric simulation chambers used in this thesis*

	<b>G-FROST</b>	<b>PAM</b>	<b>Go:PAM</b>	<b>SAPHIR</b>
<b>Material</b>	Pyrex	Metal	Quartz	FEP-Teflon
<b>Dimensions</b>	i.d: 10cm, l:191cm	d:44 cm, l: 46 cm	i.d: 9.6cm, l:100cm	270 m <sup>3</sup>
<b>Typical residence times</b>	240 s	100 s	37 s	Hours to days
<b>Chemistry</b>	O <sub>3</sub>	OH	OH	OH/O <sub>3</sub>
<b>Temperature control</b>	Controlled temperature	No temperature control	Stable temperature	Ambient
<b>OH exposure</b>	n.a.	4×10 <sup>11</sup> molecules cm <sup>-3</sup> s <sup>-1</sup>	4×10 <sup>11</sup> molecules cm <sup>-3</sup> s <sup>-1</sup>	Ambient
<b>Radiation</b>	n.a.	183 nm and 254 nm	254 nm	Sunlight
<b>Paper</b>	I, II, III	II, III	V	IV



### 3.1.1 O<sub>3</sub> as primary oxidant: G-FROST

The Göteborg Flow Reactor for Oxidation Studies at low Temperature (G-FROST) is used to study oxidation of biogenic precursors mainly with ozone as the primary oxidant. G-FROST is a flow reactor mounted vertically in a temperature controlled housing, and is described in detail in Jonsson et al (2006). Briefly, G-FROST consists of a 191 cm long Pyrex® glass cylinder with a diameter of 10 cm. VOCs and oxidant are added continuously through separate lines and allowed to react in a well-defined mixing region of the glass cylinder. The continuous flow through the reactor creates a stable aerosol output, and imposed changes to the chemistry can be monitored and analyzed. Temperature, humidity, residence time as well as the concentration of ozone and the SOA precursor can be varied with precise control. The temperature may be set and kept stable from -30° C to above 30° C. The residence time can be controlled by adjusting the position of the slider and the flows. In these studies, the residence time was 240 s calculated as plug flow.

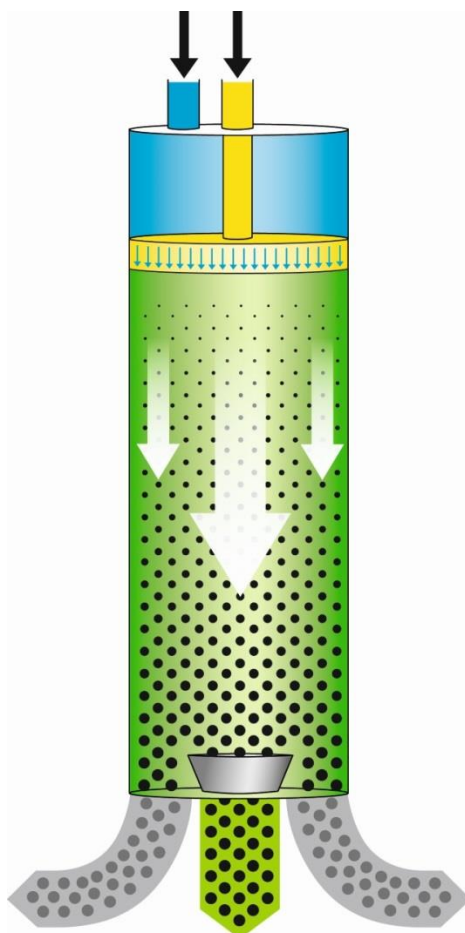


**Figure 3.1** *Illustration of G-FROST*

### 3.1.2 OH as primary oxidant: PAM and Go:PAM

The two OFRs using OH as the primary oxidant used in this thesis are shown in Figure 3.2: (i) Go:PAM, a quartz flow reactor (l: 100 cm, r: 4.8 cm) and (ii) the PAM chamber, a metal chamber (l: 46 cm, r: 22 cm). The PAM chamber was introduced by Kang et al (2007) and is described in detail elsewhere [Kang et al., 2007; Kang et al., 2011; Lambe et al., 2011], but since Go:PAM was developed as part of this thesis, it will be discussed in more detail.

As illustrated in Figure 3.2, the flows in the two OFRs are controlled in a similar way. In the experiments in this thesis, the sample flow was added to the center of the flow reactor and the oxidant flow with O<sub>3</sub> and humidified air distributed across the reactor area to improve the mixing. In PAM, the oxidant flow was introduced through a system of perforated tubes and in Go:PAM, a perforated plate was used to distribute the oxidant flow across the tube cross section and facilitate mixing of the sample. The exiting flows are controlled by the processed sample flow, sampled by the instruments, and an exhaust flow. Only the central part of the flow is sampled to reduce wall interactions. To set the total flow, three of the four flows were controlled and the fourth was open to ambient and thereby closing the mass balance.

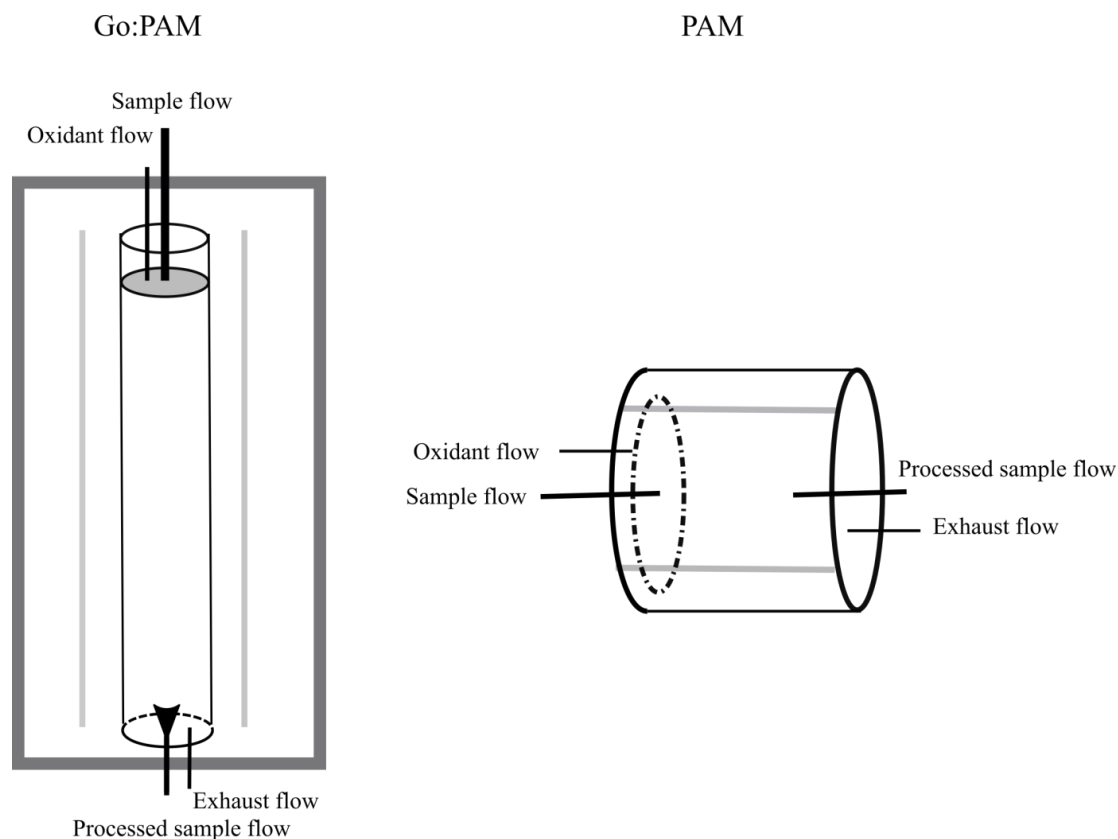


**Figure 3.2** Schematics of Go:PAM and PAM

Flow profile, residence time, flow mixing and particle loss are important characteristics of an OFR. The flow profile and residence times was studied in the two OFRs by conducting tests with CO<sub>2</sub>. By comparing Figure 3.4 and Figure 3.5, it can be seen that the residence time distribution is broader in PAM compared with Go:PAM. Furthermore, as can be seen from Figure 3.4, the response time and refresh time of PAM is long which gives limitation when studying rapidly changing emissions sources. In contrast, as is seen in Figure 3.5, Go:PAM has both a short refresh and response time. The residence time distributions of Go:PAM using a total flow of 10.13 lpm is shown in Figure 3.3. From these measurements it was found that the time for first detection of CO<sub>2</sub>, the median CO<sub>2</sub> residence time and the time from injection until the concentration had dropped below 5% of maximum were 20, 37 and 92 s, respectively. The median residence time was used as the contact time in the chemical model in Paper V. To ensure good mixing of the sample flow and oxidants flow, tests were conducted by adding SO<sub>2</sub> in the two inlets in turn, and from Figure 3.6 it can be seen that the flows are well-mixed in Go:PAM.

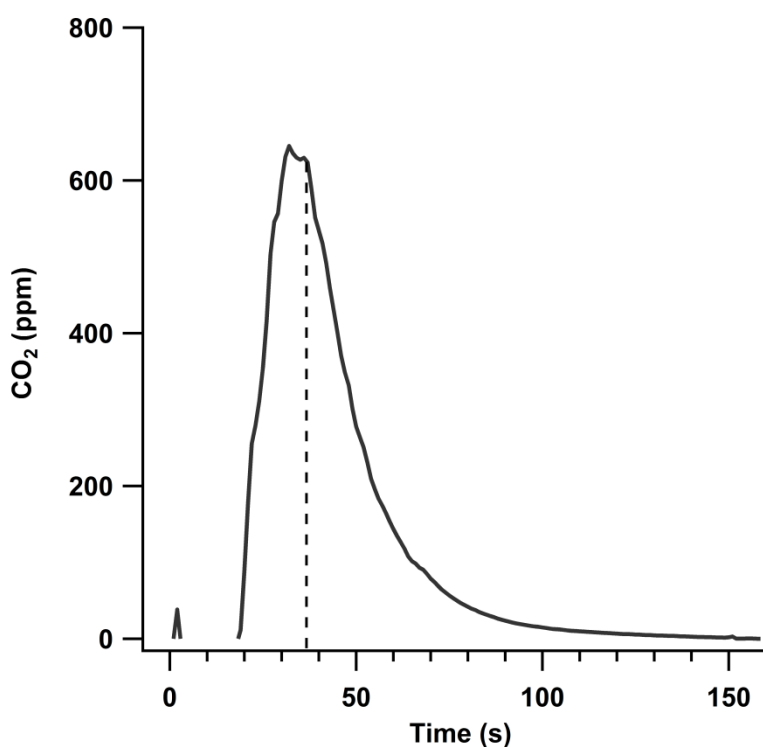


**Figure 3.3** The residence time distribution of Go:PAM. The contact time used in the chemical model is indicated. The small peak at 4 s indicate time of introduction of a 5s square pulse of CO<sub>2</sub>.

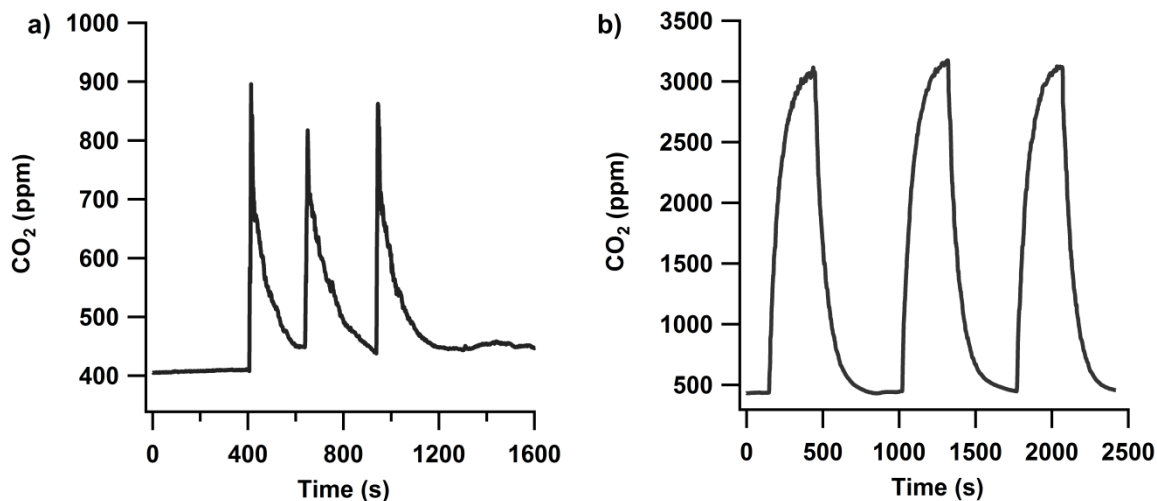


Figure 3.4 Flow profile of CO<sub>2</sub> pulses to PAM a) 10 s b) 5 min

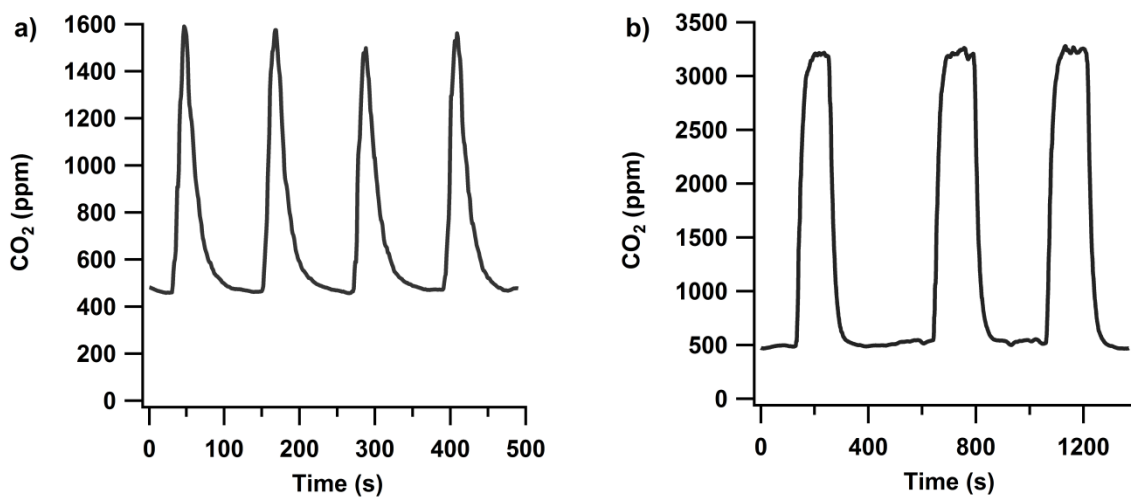


Figure 3.5 Flow profile of CO<sub>2</sub> pulses to Go:PAM of a) 10 s b) 120-150s.

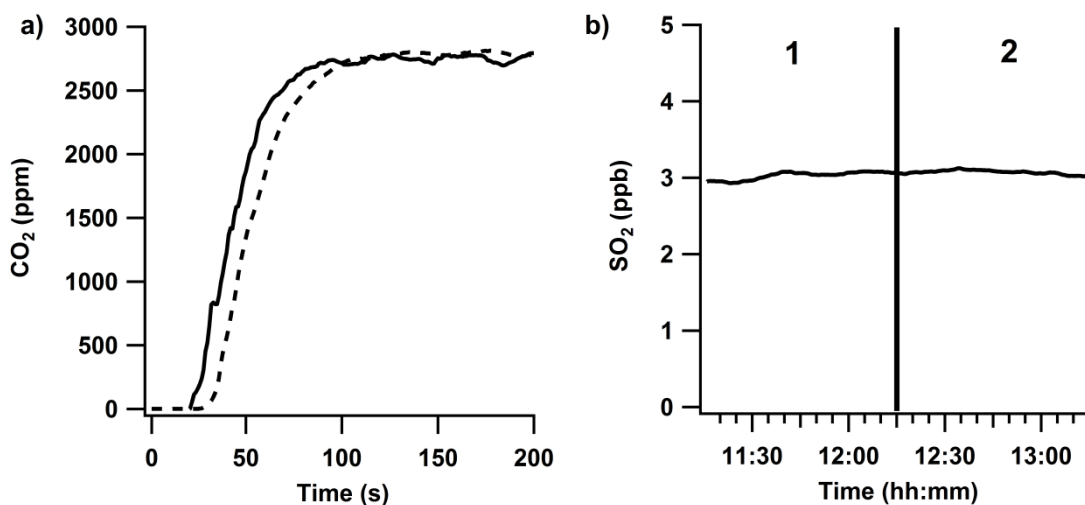
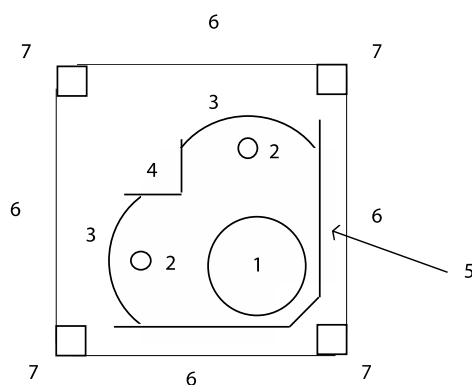


Figure 3.6 (a) Concentration of CO<sub>2</sub> simultaneously measured in processed sample flow (solid) and exhaust (dashed) and (b) concentration of SO<sub>2</sub> added in turn in the oxidant flow (1) and sample flow (2).

Some particle loss in OFRs is inevitable. However, studies have found general small losses in PAM, but with increased importance at smaller sizes [Karjalainen et al., 2016b; Lambe et al., 2011]. The design of Go:PAM further limits particle wall losses by the flow tends to develop into a laminar flow after initial mixing and by only the central part is sampled to the instruments. This restricts contact of the aerosol sample with the wall, and reduces particle loss by diffusion. Regarding the particle loss, the system has been used with a CPC as a reference point parallel to the EEPS. The EEPS to CPC relationships without Go:PAM was 0.97, while if the EEPS sampled after Go:PAM it was reduced to 0.93. Nevertheless, for this work particle loss is of minor importance, especially since the focus is on relative changes, and consequently these losses were neglected in the analysis.

An important feature of many OFRs is the possibility to produce OH radicals. In PAM and Go:PAM, OH radicals are formed from photolysis of ozone at 254 nm and subsequent reaction of  $O(^1D)$  with water (R2.6-2.7). PAM is equipped with two UV lamps (BHK Inc) which produce light with wavelengths of 185 nm and 254 nm which enables production of both  $O_3$  and OH. In this work, however, the lamps were mounted inside Teflon-coated quartz sheaths, which blocked the transmission of 185 nm light, and  $O_3$  was produced up-streams by an ozone generator. A horizontal cross section of Go:PAM is shown in Figure 3.7. The reactor is equipped with two 10W UV lamps with wavelengths of 254 nm (Phillips TUV 30 W). The photon flux onto the reactor is enhanced by two 90 cm long parabolic reflectors, one situated behind each lamp. Furthermore, to reduce the inhomogeneity of the photon field, the tube is enclosed in a compartment of flat aluminum mirrors.



**Figure 3.7** Horizontal section of the Go:PAM reactor. 1) 9.6 cm id quartz tube 2) UVC fluorescent tube 3) Parabolic trough mirror 4) 90 deg. flat mirror 5) 45-90 deg. flat mirror 6) sheath metal cover 7) Square tubing support structure. Graphic design by Evert Ljungström. Printed with permission.

The production of OH radicals can be varied by changing water and O<sub>3</sub> concentration as well as photon flux and residence time. Since the absolute concentration of OH radicals is difficult to measure and determine, the OH exposure is a key parameter for data interpretation. The OH exposure can be defined as the integral of the time-dependent OH concentration over the time that the sample is exposed to OH radicals. Ideally, the OH exposure should be measured continuously, but it is a challenge to find the right compound for this purpose. Therefore, the OH exposure often is estimated in separate experiments by indirectly determine the decay of a known concentration of gas (e.g SO<sub>2</sub>, CO, formic acid) due to the reaction with OH radicals.

$$OH \text{ exposure} = \frac{1}{k_{OH+gas}} * -\ln\left(\frac{gas_f}{gas_i}\right) \quad (\text{Eq 3.1})$$

where  $k_{OH+gas}$  is the rate constant between the used compound and OH, and  $gas_f$  and  $gas_i$  is the final and initial gas concentration, respectively. In this work, the OH exposure was determined by measuring the decay of SO<sub>2</sub> from the reaction with OH radicals.

In a OFR where OH is produced from photolysis of O<sub>3</sub>, non- OH reactions can take place since the sample is illuminated by UV light. Aromatic substances can absorb UV light, and therefore the photolysis can influence the chemistry in the OFR. It is known that traffic emit aromatic compounds [Dunmore et al., 2015]. Toluene is one example of an aromatic compounds emitted from traffic, and to determine the importance of photolysis of toluene in Go:PAM, the relative photolysis fraction can be calculated according to Eq. 3.2.

$$Relative \text{ photolysis fraction} = \frac{Photolysis \text{ rate at } 254 \text{ nm}}{(Photolysis \text{ rate at } 254 \text{ nm} + \text{reaction rate with OH})} \quad (\text{Eq. 3.2})$$

Given the calculated actinic flux in Go:PAM and assuming unity quantum yield, the relative photolysis rate of toluene in Go:PAM at the highest OH exposure was about 1 %. This indicates that the main reaction of toluene is the reaction with OH radicals. To investigate the possible photolysis of aromatics further in Go:PAM, flows containing toluene and trimethyl-benzene were exposed to the lights in the Go:PAM, and no sign of reduction of these aromatics were observed when turning on the UV-lights. This indicates that the chemistry in Go:PAM is driven by OH oxidation, and that the flow reactor can be used to study atmospheric relevant aging processes.

### 3.1.3 Experimental set-up in the monoterpenes experiments

Figure 3.8 summarize the experimental set-up and aerosol characterization used in Paper I-III. In Paper I, only G-FROST was used, and in Paper II and III, a combination of G-FROST and PAM were used. The aerosol was characterized by particle size distributions in all papers. There was a focus on the thermal properties of the aerosol particles in Paper I-II, whereas in Paper III the focus was on the chemical composition of the aerosol.

All experiments were started by adding the monoterpenes together with water, and in some cases also OH scavenger, and the system was allowed to stabilize, often overnight. The monoterpenes (and in some cases OH scavenger) were delivered to the flow reactors by letting a flow of N<sub>2</sub> pass the open end of a diffusion tube which was kept a stable temperature, and the temperature controlled the concentration of precursors. As the oxidant was added, the aerosol production started, and the aerosol characterization started when a stable production was achieved. Whenever there was a change to the system, the system got time to stabilize before the aerosol was characterized.

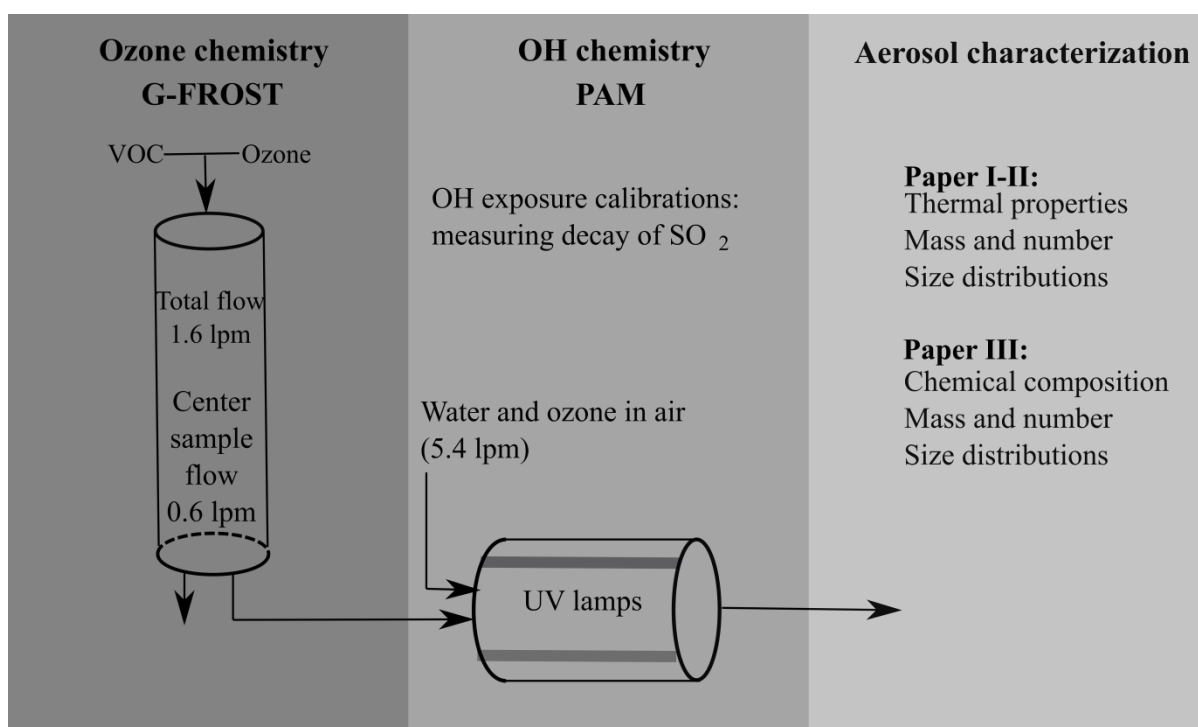


**Figure 3.8** Schematic of the experimental set-up used in Paper I-III.

## 3.2 Atmospheric simulation chambers

There are several atmospheric simulation chambers around the world varying in size, shape and material, all with their benefits and drawbacks. SAPHIR, hosted by Forchungszentrum Julich, is among the largest simulation chambers. The size of SAHIR enables studies of longer time scales, and reduces particle losses due to low surface to volume ratio.

### 3.2.1 SAPHIR

SAPHIR, shown in Figure 3.9, can be used for low concentration experiments close to ambient conditions. It is a 270 m<sup>3</sup> cylindrical chamber of double walled FEP-Teflon. The Teflon allows natural solar radiation to penetrate and enables studying atmospheric photo oxidation by natural sun light. The chamber is kept under a constant pressure of 40 Pa above ambient, so 15 m<sup>3</sup> h<sup>-1</sup> of clean air is added in order to compensate for sampled air and small leaks. SAPHIR is equipped with a suite of analytical instruments for particle and gas measurements as well as for physical parameters.



**Figure 3.9** *The atmospheric simulation chamber SAPHIR. (Photo: Eva Emanuelsson)*

The experiments in the SAPHIR chamber were initiated by adding the precursors to a clean, humidified and dark chamber. The precursors were allowed to stabilize before ozone was added, and immediately after the ozone addition, the roof was opened and the photo-oxidation started. The roof was closed in the evening and opened again in the morning. The aerosol, both gas and particle phase was continuously characterized, and in addition, during the final 2 hours each day, a more detailed characterization of the thermal properties of the aerosol particles were conducted.



### 3.3 Fuel related emission factors

Emission factors are a fundamental tool in inventories for air quality management and decision making. It relates pollution to an associated activity, e.g number of CO<sub>2</sub> molecules emitted per km driven or kilogram fuel burnt. In Paper V, fuel specific particle emissions factors were derived from extractive sampling from the exhaust plumes of in-use buses. The measurements were conducted according to Hallquist et al (2013), and the experimental set-up is shown in Figure 3.10a.

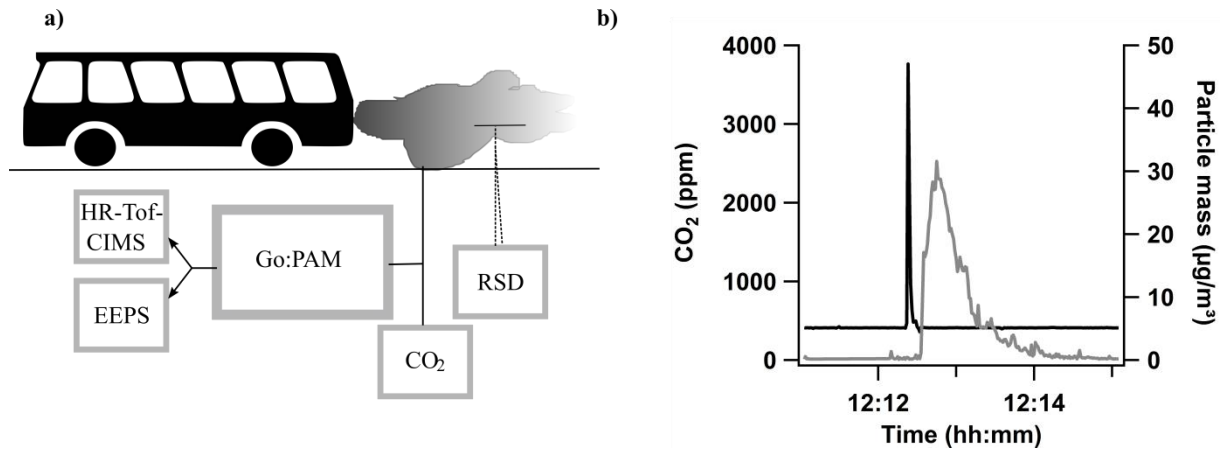


**Figure 3.10** a) Schematic figure of the set-up and b) example of changes in CO<sub>2</sub> (black) and particle mass (grey) concentration when a bus passes the sampling inlet. RSD (Remote Sensing Device), EEPS (Engine Exhaust Particle Sizer), HR-ToF-CIMS (High Resolution Time-of-Flight Chemical Ionization Mass Spectrometer), Go:PAM (Gothenburg Potential Aerosol Mass reactor).

As can be seen in Figure 3.10 b, the concentration of CO<sub>2</sub> and particles increase from their background values as a bus passes the sampling inlet. From the time integrated background corrected concentration changes, the fuel specific particle EF can be calculated according to Equation 3.2.

$$\text{Fuel specific } EF_{part} = \left( \frac{\Delta_{particles}}{\Delta CO_2} \right) EF_{CO_2} \quad (\text{Eq 3.2})$$

where  $\Delta_{particles}$  and  $\Delta CO_2$  are the background corrected time integrated concentrations of particles and CO<sub>2</sub>, respectively. In the calculations complete combustion is assumed, i.e. the emitted CO<sub>2</sub> is assumed to be directly proportional to the fuel consumption. Furthermore, a carbon content of 86.1, 77.3 and 69.2 % for diesel, RME and CNG, respectively, were assumed [Edwards et al., 2014].

## **4. Aerosols characterization**

Changes in particle size distributions and particle concentrations give insight in processes important for formation and aging of secondary aerosols. Particle concentration and size distributions have been measured in all papers in this work (Paper I-V). In this work there has been a special focus on the thermal properties of the aerosol particles Paper (I-IV), measured with a Volatility Tandem DMA (VTDMA), and an evaluation method for data from the VTDMA was developed during the course of this work. In addition, the chemical composition of the secondary aerosol has been studied (Paper III).

### **4.1 Particle number concentration and particle size distributions**

The particle number concentration and particle size distribution provide information on the properties of aerosol particles, and monitoring changes are often of great interest when studying atmospheric aerosols. A Condensation Particle Counter (CPC) measures the particle number concentration continuously and online. The CPC consists of three main parts. The first part is a flow through chamber where the air is saturated with a suitable compound (in this work 2-butanol) at a slightly increased temperature. Then, the particles enter a cooled part where the gas becomes supersaturated and the 2-butanol will condense onto the particles and the particles will grow into sizes that can be detected optically. The last part is an optical laser based-device that counts the particles. A differential mobility analyser (DMA) is used to create a monodisperse aerosol from a polydisperse aerosol. Simplified, the DMA consists of a metal cylinder with a charged rod inside. The charged rod creates an electrical field in the DMA and depending on their electrical mobility particles travel at different speeds in the electrical field. Particles with a chosen electrical mobility will exit the DMA as a monodisperse aerosol. By scanning over electrical field strengths in the DMA and using a CPC as a detector, it is possible to measure a particle size distribution. The combination of a DMA and CPC is known as a Scanning Mobility Particle Sizer (SMPS).

The SMPS needs a relative long time to capture data with high size resolution, and therefore the instrument is not suited to measure size distributions from rapidly changing emission sources. In order to measure real-time particle number concentrations and size distributions from a rapidly changing emission source, an Engine Exhaust Particle Sizer Spectrometer (EEPS) can be used. The EEPS measures instantly a full size distribution. The particles are separated by their electrical mobility in the EEPS column and are detected by the induced current on 22 electrodes in the EEPS column which enables measuring a particle size distribution from 5.6 to 560 nm with up to 10 Hertz resolution.

To calculate size and mass from the methods described above the assumptions on shape and density of the particles are required. The density of SOA particles must be estimated when there is no direct measurement available, and in Paper I-IV, the SOA particles are assumed to be spherical with a density of  $1.4 \text{ g cm}^{-3}$  [Hallquist et al., 2009]. Exhaust particles are geometrically very complex, and the constituent is often unknown, so for comparative purposes, unity density and spherical particles were assumed for all exhaust particles in Paper V.

## 4.2 Thermal properties

A volatility tandem DMA (VTDMA) has been used in this work to study the thermal properties of SOA (Figure 4.1). The VTDMA is described in detail elsewhere [Jonsson et al., 2007; Salo et al., 2010], and will only be presented briefly here. The general idea is to let monodisperse particles, selected in the first DMA, evaporate in a heating unit and changes in size of the particles is monitored by a SMPS. The heating unit consists of 8 parallel 50 cm long ovens which can be set at temperatures from room temperature and up to 573 K. The residence time in the ovens is  $\sim 2.8 \text{ s}$ . In order to avoid re-condensation of the evaporated gases upon cooling, the aerosol is sent through charcoal denuders before the SMPS system measures the residual particle size distribution.

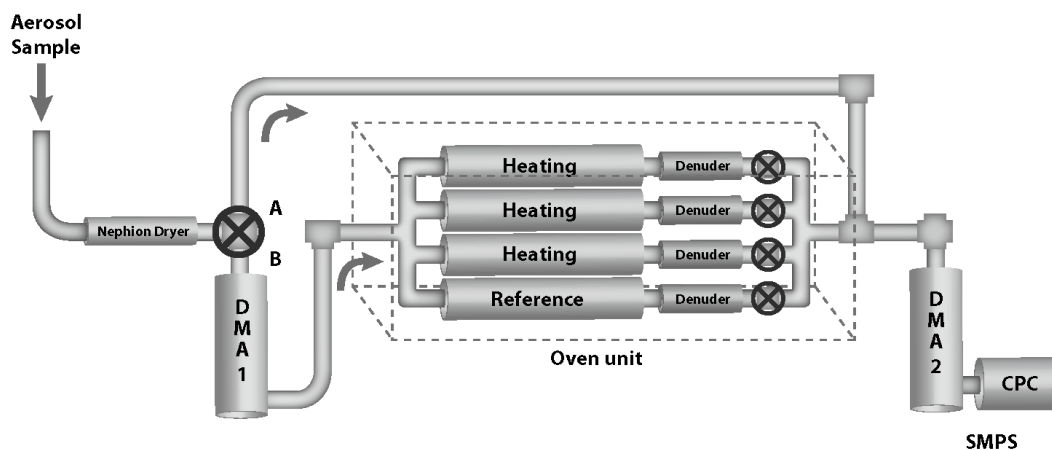


**Figure 4.1** Schematic of the VTDMA system. Graphic design by Eva Emanuelsson. Printed with permission.

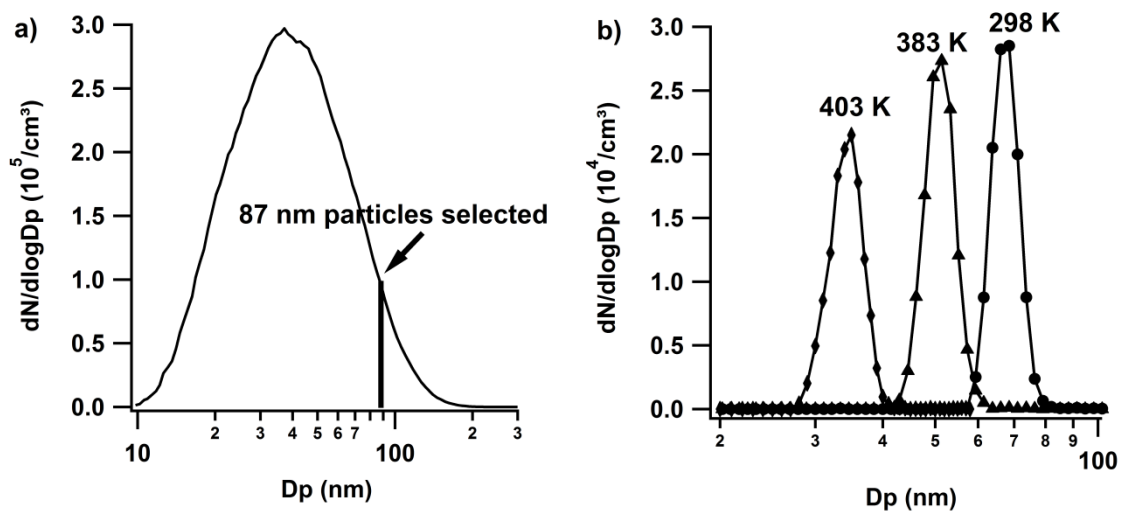


**Figure 4.2** Example of the VTDMA method. (a) Initial number size distribution. (b) Residual number size distribution after selection with the first DMA and evaporation in the oven unit at three temperatures (298, 383, 403 K)

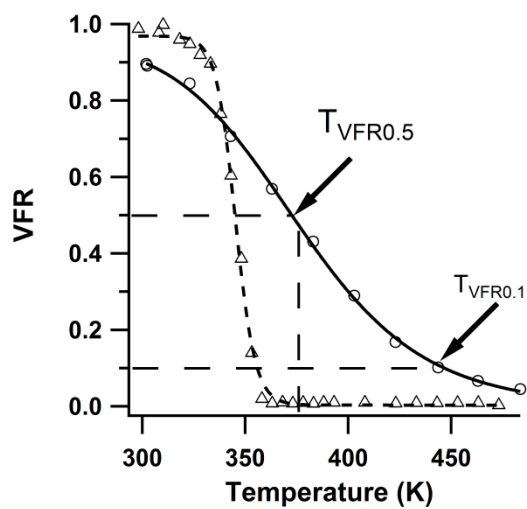


**Figure 4.3** Thermogram of pure pinonic acid particles (dashed) and oxidized  $\alpha$ -pinene SOA (solid)

Figure 4.2 shows an example of data obtained from the VTDMA. The peak median size of the residual size distribution ( $D_{pr}$ ) is normalized to the size of the reference selected by the first DMA ( $D_{pref}$ ) and from this the volume fraction remaining (VFR) is calculated using Equation 4.1

$$VFR = \left( \frac{D_{pr}}{D_{pref}} \right)^3 \quad (\text{Eq 4.1})$$

In order to capture more details about the thermal properties of particles, VFR can be measured for a range of temperatures for the same aerosol, and a so-called thermogram can be generated. Examples of thermograms for two different types of aerosols are shown in Figure 4.3. However, qualitative analysis of thermograms by simply comparing them is difficult, and therefore to enable better analysis of the VTDMA data, a method using a sigmoidal curve fit to the data was developed. The thermograms were fitted to the Equation 4.2

$$VFR_T = VFR_{min} + \frac{(VFR_{max} - VFR_{min})}{1 + \left( \frac{T_{position}}{T} \right)^{S_{VFR}}} \quad (\text{Eq 4.2})$$

where the exponent,  $S_{VFR}$ , describes the steepness of the curve and  $T_{position}$  determine the mid position of the curve.  $VFR_{max}$  and  $VFR_{min}$  set the boundaries of the highest and the lowest VFRs, respectively. In order to obtain the best fit to the data  $VFR_{max}$  and  $VFR_{min}$  are not restricted *a priori*. In Paper I, II and IV,  $T_{VFR0.5}$ , i.e an indicator of the general volatility which is the temperature where 50% of the particle volume has evaporated and the exponent,  $S_{VFR}$ , determines the steepness of the curve and is a measure the aerosol constituents volatility distribution. Furthermore, in Paper I, the semi volatile fraction of the aerosol particle was defined as the VFR at 298K ( $VFR_{298}$ ) and in Paper III, the temperature where VFR was 0.1,  $T_{VFR0.1}$ , was used as an indicator for least volatile fraction of the aerosol particles.

### 4.3 Particle chemical composition

The atmospheric concentration of many of the organic compounds in is very low. Filter sampling enables sampling of large volumes of air which permits identification and quantification of compounds of low concentration. Freshly formed  $\alpha$ -pinene SOA were sampled by a filter/denuder system and analyzed for their content of organic acids and dimer esters in Paper III. The method is described in detail in elsewhere [Kristensen et al., 2016; Kristensen et al., 2014] and will only be briefly described here. The particle phase of the freshly formed SOA was sampled with a low-volume sampler (LVS) denuder/filter sampling system. This allowed simultaneously capturing and hence separation of gas and particle phase. The samples were analyzed by using an ultra-high-performance liquid chromatograph coupled to the electrospray ionization source of a Bruker Daltonic quadrupole time-of-flight mass spectrometer (UHPLC/ESI-QTOF-MS) operated in negative ionization mode. The details on the extraction of the samples as well as operating conditions of the mass spectrometer are described in Kristensen et al (2016).

### 4.4 Supporting measurements

In this work, gas measurements provide important supporting information, and most of the gas measurements were done using standard continuous online methods: the ozone concentrations were measured using an UV photometric method, SO<sub>2</sub> was measured using UV fluorescence method, CO<sub>2</sub> was measured using a non-dispersive infrared gas analyzer. In addition in Paper IV, the VOC concentration in the gas phase was monitored using a Proton Transfer Mass spectrometer (PTR-MS). The proton transfer is a soft ionization method and can be used to detect unsaturated hydrocarbons (e.g. monoterpenes), aromatic hydrocarbons (e.g. benzene) and most oxygenated hydrocarbons. Furthermore in Paper IV, the concentration of OH radicals were measured using the Differential Optical Absorption Spectroscopy (DOAS) technique. In Paper V, a remote sensing device (RSD) was used to measure NO, HC and CO. In Paper VI, the chemical composition of the aerosols particles was measured using Aerosol Mass Spectrometers (AMS).

## 5. Results and discussion

In this work formation and aging from oxidation of atmospheric relevant precursors has been studied. Oxidation chemistry of selected biogenic compounds, oxidation agents and their effect on the thermal properties of secondary organic aerosol were studied in Paper I-IV. In Paper V, emissions from in-use transit buses were aged by exposing the plumes to high concentration of OH radicals.

### 5.1 Oxidation of biogenic emissions

The formation and properties of SOA formed from ozone and OH induced oxidation of  $\alpha$ -pinene,  $\beta$ -pinene and limonene was studied in Paper I-III by detailed laboratory studies.

#### 5.1.1 Radical chemistry and water concentration

In Paper I, the effect of humidity and the radical chemistry on the ozonolysis of  $\beta$ -pinene was studied in detail. A negative humidity effect on particle mass and number on the SOA produced by  $\beta$ -pinene ozonolysis was observed. As can be seen in Figure 5.1, water is directly involved with SCI in the formation of nopinone (R3a). Nopinone is believed to not contribute to particle mass due to its low partitioning coefficient [Hohaus et al., 2015]. The humidity did not only affect the mass and number concentration for  $\beta$ -pinene SOA formed, but also the thermal properties of the SOA were affected. Generally, a less volatile SOA was formed from  $\beta$ -pinene oxidation at lower humidity compared with higher water concentration. From Figure 5.1 (R3a and R3b) it can be seen that at lower humidities more of the SCIs will react with a carbonyl forming a secondary ozonide (SOZ). Nopione, which also is formed from the initial decomposition of the primary ozonide (POZ), can react with SCI and a C<sub>18</sub>-SOZ is formed (Figure 5.2). This C<sub>18</sub>-SOZ has low vapor pressure and can facilitate nucleation and contribute to SOA mass. The humidity effect on SOA formed from ozonolysis of  $\beta$ -pinene is opposite compared to SOA formation from ozonolysis of  $\alpha$ -pinene and limonene [Jonsson et al., 2008b; Jonsson et al., 2008a]. In the ozonolysis of  $\alpha$ -pinene, an increased humidity will lead to an increased production of acids that can lower the particle volatility and enhance particle formation [Jonsson et al., 2008a; Jonsson et al., 2007].

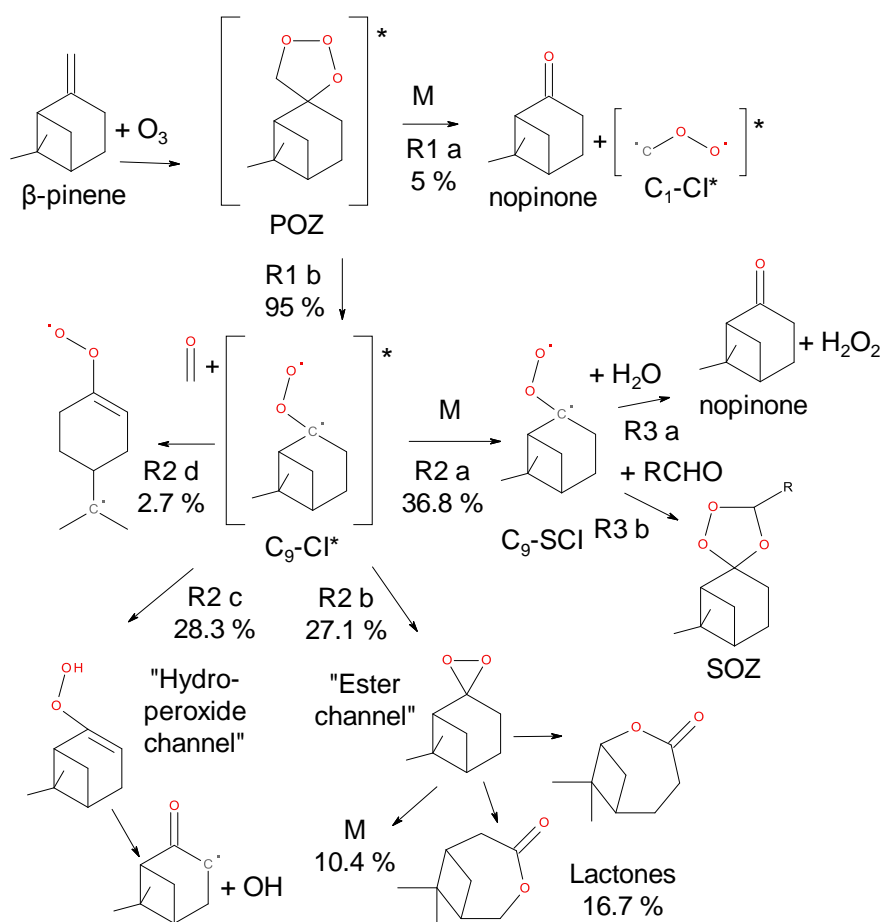


**Figure 5.1** Major reaction paths in the ozonolysis of  $\beta$ -pinene. The routes and yields were taken from [Nguyen et al., 2009] omitting isomers and paths with yields below 1%. The reactions of the SCI (R3 a and R3 b) were suggested by [Winterhalter et al., 2000].

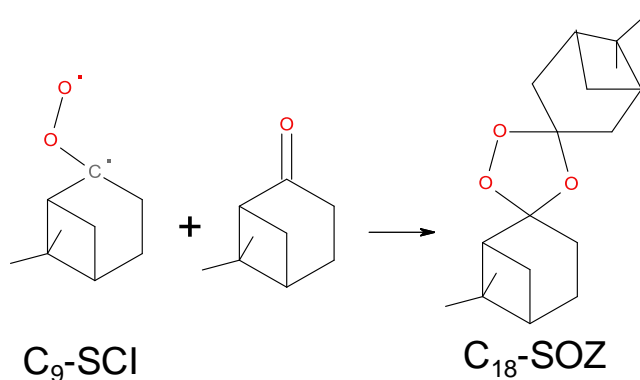


**Figure 5.2** Formation of  $\text{C}_{18}\text{-SOZ}$  from the reaction of the  $\text{C}_9\text{-SCI}$  and nopinone, starting from the SCI channel shown in Figure 5.1.



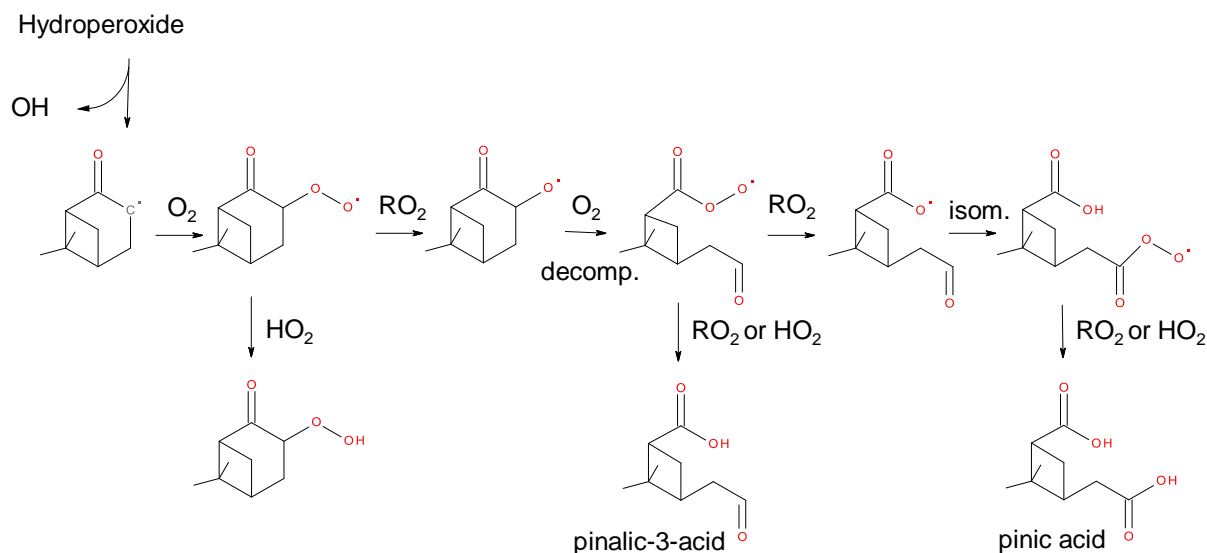


**Figure 5.3** Formation of multifunctional oxygenated products by a sequence of radical reactions of  $\beta$ -pinene, starting with the alkyl radical from hydroperoxide channel shown in Figure 5.1.

The combined effects of changes in radicals and humidity observed in Paper I could not be fully explained by the major reaction paths in the ozonolysis of  $\beta$ -pinene shown in Figure 5.1. However, in the literature it has been suggested that SCI can rearrange into a hydro peroxide [Drozd et al., 2011; Nguyen et al., 2009; Zhang and Zhang, 2005]. This reaction will directly compete with water and could explain the water effect observed in Paper I. Furthermore, for hydro peroxides, as can be seen in Figure 5.3., there will be a competition between  $HO_2$  and  $RO_2$  with  $HO_2$  terminating the radical chain reactions. In Paper I it was shown an increased SOA production with decreased  $HO_2/RO_2$  ratio. The SOA formed with a low  $HO_2/RO_2$  ratio was generally less volatile compared to the SOA formed from with a higher ratio. It can be seen from Figure 5.3 that higher concentration of  $RO_2$  favor production of carboxylic acids which can enhance particle growth and reduced particle volatility. Notably,  $RO_2$  concentration had no or small effect on the volatility of  $\beta$ -pinene SOA formed when the humidity was high which indicates that the production of nopinone is favored even with high concentrations of  $RO_2$ . This is supported by increased high humidity leads to formation of a less complex aerosol. In summary, the SOA production from the ozone-induced oxidation of  $\beta$ -pinene is sensitive to changes in humidity with less and more volatile SOA formed with increasing humidity.

### 5.1.2 Formation of dimer esters

Dimer esters contributed 5-16 % of the freshly formed SOA mass formed from ozonolysis of  $\alpha$ -pinene (Paper III). Although no dimer esters were observed in the gas phase it is likely that they are formed through gas phase reactions due to their low vapor pressures and the short reaction time. This highlights their potential to be important for new particle formation. Recently, the gas phase production of these compounds have been supported by recent subsequent ambient observations [Mohr et al., 2017] and more laboratory studies [Kourtchev et al., 2016; Zhang et al., 2017].

The level of dimer esters was lower from the OH induced oxidation compared to the  $O_3$  induced oxidation experiments which indicates that ozone is required in the initial formation. In Paper III, the suggested mechanism for this formation involves a reaction with a SCI and an oxygenated organics (e.g. carboxylic acid). There has also been a suggestion for dimer esters formation from the  $RO_2$  self-reaction [Zhang et al., 2015], with this reaction becoming more important at higher VOC concentrations [Kourtchev et al., 2016]. In experiments in Paper III it was found, however, that the concentration of the most abundant dimer esters increased with an increased  $HO_2/RO_2$  ratio. This indicates that these dimer esters are formed from the reactions involving SCI and oxygenated organics. Moreover, the concentration of 20 of the 28 identified dimer esters decreased with increased  $HO_2/RO_2$  ratio, and for these compounds formation through the  $RO_2$  self-reaction can be the dominating reaction path. Based on these results it is possible to speculate that in the ambient atmosphere both suggested formation paths are available. This is further supported by recent ambient measurements of dimer esters [Mohr et al., 2017].

The experiments in Paper III were done using  $\alpha$ -pinene as a SOA precursor, but in principle could same reaction paths be available for other monoterpenes. For example, in the  $\beta$ -pinene ozonolysis, as already discussed and shown in Figure 5.2, a higher concentration of  $RO_2$  will increase the formation of carboxylic acids. The acids formed can then be available for the reaction with SCI which in turn can lead to the formation of dimer esters. Furthermore, high concentration of  $RO_2$  will also enhance the  $RO_2$  self-reaction which also can enhance to the formation of dimer esters. This formation is supported by observations of dimers in the dry ozonolysis experiments with  $\beta$ -pinene with low  $HO_2/RO_2$  ratio [Kolesar et al., 2015]. Although the ambient concentration of these compounds probably is low, they can be of importance due to their ability to form new particles.

### 5.1.3 Thermal properties of freshly formed SOA

The oxidation conditions affect the formation of monoterpene SOA, and this was studied in Paper I and II. An increased extent of OH based oxidation of  $\alpha$ -pinene,  $\beta$ -pinene and limonene increase the volatility, seen as a decreased  $T_{VFR0.5}$ , and complexity, seen as increase in  $S_{VFR}$ , of the SOA formed. Products formed from the ozonolysis can have higher addition of oxygen to the molecule, and therefore a larger degree of functionalization and lower volatility. The use of OH scavenger reduces the number of available reactions paths, and by that limit the number of products that can be formed. In contrast, with increased the OH exposure the number of available reaction channels will increase which will lead to broadening of the volatility distribution.

In Paper II it was shown that SOA produced from ozonolysis of limonene is generally less volatile than SOA produced from ozonolysis of  $\alpha$ -pinene and  $\beta$ -pinene. This is in accordance with previous reported findings on volatility of  $\alpha$ -pinene and limonene SOA [Jonsson et al., 2007; Kolesar et al., 2015; Lee et al., 2011]. Furthermore, as can be seen in Figure 5.5b, the fraction of the least volatile compounds ( $T_{VFR0.1}$ ) was also higher in ozone induced limonene SOA compared to the fraction in SOA formed from ozonolysis of  $\alpha$ -pinene and  $\beta$ -pinene. These findings are in line with recent studies on formation of ELVOC from monoterpene oxidation [Ehn et al., 2014; Jokinen et al., 2015]. Furthermore, limonene SOA is more complex compared to  $\alpha$ -pinene and  $\beta$ -pinene SOA. The difference between limonene and the pinenes can to a large extent be explain by the fact that limonene has two double bonds which makes it possible for oxidants to react with both double bonds. This allows formation of a wider range of products with higher functionalization. Furthermore, it was found that there is no major difference in the volatility of the ozone induced SOA formed from  $\alpha$ -pinene and  $\beta$ -pinene, which is in line with the results of Kolesar et al (2015) and Lee et al (2010). Recently, laboratory studies found formation of terpenylic acid and  $C_9H_{14}O_5$  compounds in SOA formed from the ozonolysis of  $\alpha$ -pinene and  $\beta$ -pinene [Sato et al., 2016], which can be an explanation to why there is no major difference in the volatility of ozone induced SOA from  $\alpha$ -pinene and  $\beta$ -pinene.

The difference in complexity between pure ozone induced SOA and ozone induced SOA with an influence of OH radicals was smallest for limonene. This indicates that the relative influence of the OH chemistry is more important for  $\alpha$ -pinene and  $\beta$ -pinene than for limonene. For the pinenes, an enhanced OH exposure will lead to formation of more products which can contribute to particle formation and condensational growth. Limonene is less sensitive for increase of OH radicals since the products formed from the ozonolysis of limonene are already efficient in particle production [Jonsson et al., 2007].

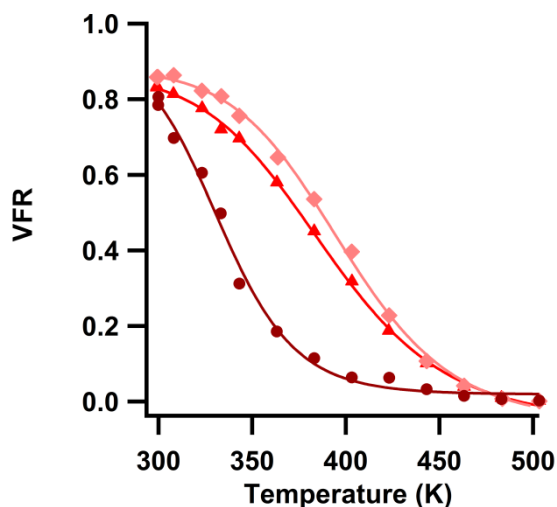


**Figure 5.4** The VFR as a function of the evaporation temperature for limonene SOA in experiments with  $O_3$  as the primary oxidant (diamonds), OH as the primary oxidant (circles) and mix with both  $O_3$  and OH as oxidants (triangles). The solid lines represent the fitted function to derive  $T_{position}$  and  $S_{VFR}$ .

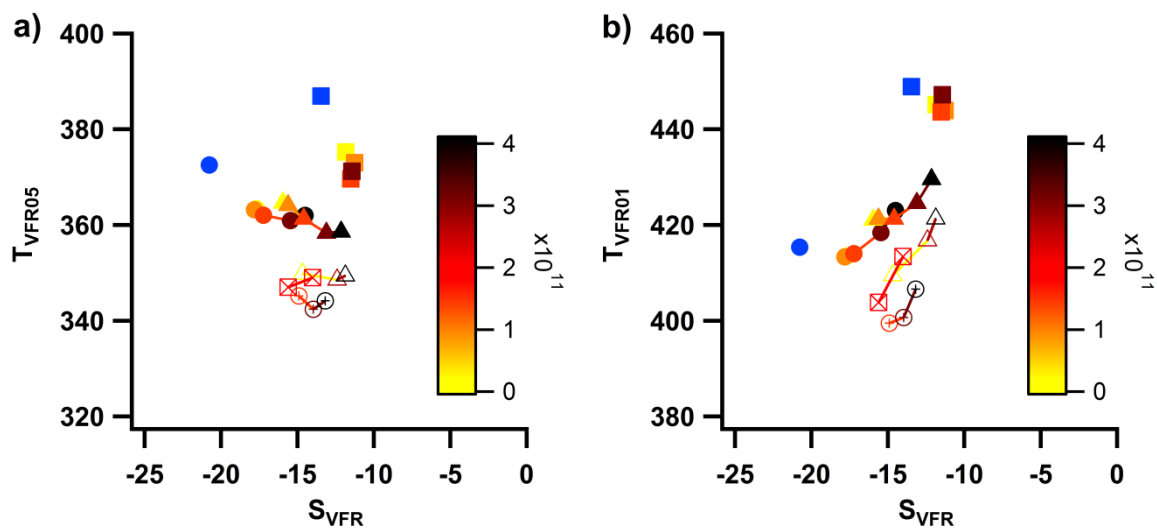


**Figure 5.5**  $T_{VFR0.5}$  (a) and  $T_{VFR0.1}$  (b) plotted as functions of  $S_{VFR}$  for  $\alpha$ -pinene (circles),  $\beta$ -pinene (triangles) and limonene (squares) in the pure  $O_3$  experiments (blue), the combined OH and  $O_3$  experiments (closed) and OH (open) experiments. Darker markers correspond to higher levels of OH exposure.

In PAM and G-FROST, independent of precursors and oxidation conditions, a substantial fraction of the freshly formed SOA was semi volatile, defined by the fraction of the particle evaporated at 298 K (Figure 5.4). Notably, the evaporation is rather an effect of dilution than of heating. As the sampled aerosol enters the VTDMA, the sample is diluted by the sheath air in the first DMA. In addition, a large fraction of the total organic mass is removed as the monodisperse aerosol is created. As can be seen from Equation 2.1, this combined dilution of both the gas phase and removal of organic particle mass in the VTDMA, will lead to evaporation of semi volatile compounds (SVOC) from the particles. There have been observations large SVOC fractions of freshly formed SOA in atmospheric simulation chamber studies containing [Donahue et al., 2012; Salo et al., 2011; Vaden et al., 2011]. However, in this work, the fraction of SVOC in freshly formed SOA in SAPHIR was masked due to a different choice of reference used in the VTMDA. To conclude, monoterpene oxidation will lead to production of compounds with a wide range of volatilities which will be important for both new particle formation and condensational growth of atmospheric particles.

## 5.2 Aging of Secondary Organic Aerosols

Atmospheric oxidative aging of SOA can be simulated by exposing precursors to increased OH exposure. The effect of oxidative aging of biogenic SOA was studied using an OFR by increasing the OH exposure (Paper II), and in an atmospheric simulation chamber by oxidation induced by natural sunlight (Paper IV).

### 5.2.1 Oxidative aging in OFRs and chambers

Aging of SOA can be studied in OFRs and atmospheric simulation chamber; however, there are important differences between the two systems. The differences can be illustrated by the changes in particle mass and number concentration in PAM and SAPHIR (Figure 5.6). In SAPHIR, where the OH exposure is accumulated during the light hours, there is an increase in particle mass and number concentrations the first three hours of the experiments, but due to dilution and deposition, the particle mass and number concentrations will decline over time. For experiments using the PAM it is a general increase in particle mass and number with OH exposure. However, in the PAM it is possible to achieve much higher OH exposures compared to in SAPHIR, and at very high OH exposures the mass concentrations in PAM can start to decline which is an indication to that fragmentation of compounds becomes more important [Kang et al., 2007; Lambe et al., 2011; Palm et al., 2016].

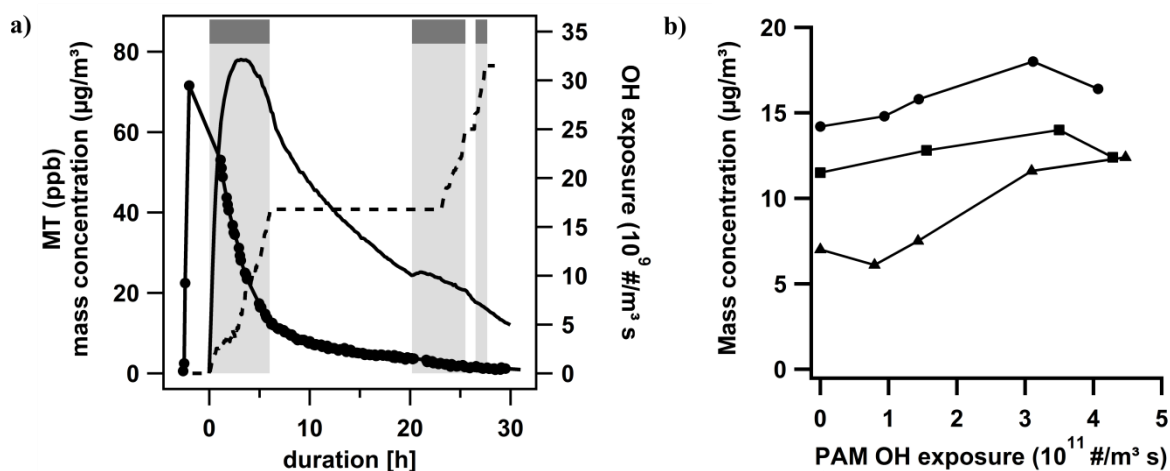


**Figure 5.6** Changes in monoterpene concentration (markers), OH dose (dashed) and particle mass concentration (solid) during one typical experiment in SAPHIR. The periods where the roof is open is indicated in grey (a), and changes in PAM particle mass concentration plotted as functions of OH-exposure for  $\alpha$ -pinene (circles),  $\beta$ -pinene (triangles), limonene (squares) (b)

As can be seen in Figure 5.7, also the thermal properties of SOA evolve differently due to aging in the two systems. In SAPHIR, the  $T_{VFR0.5}$  increased with increasing OH exposure, and it was found that the OH exposure was the major driving force for this decrease. In contrast in PAM, no change in the  $T_{VFR0.5}$  was observed with increased OH exposure. The SOA formed in PAM reflects compound distribution with a range of OH exposures, and therefore the SOA always contains a fraction of less oxidized compounds. In addition, as the total organic mass in PAM is increasing with OH exposure, more of gas-phase semi volatile compounds will partition towards the condensed phase. These combined effects lead to no change in volatility with increased OH exposure in PAM. On the other hand, as can be seen from Figure 5.5b, the fraction of lower volatile products ( $T_{VFR0.1}$ ) is increasing with increasing OH exposure in PAM which will lead to broadening of the volatility distribution. Due to the successive dilution in SAPHIR, condensed phase products can be redistributed to the gas phase, and be further oxidized into compounds with lower volatility. There will be a higher net outflow from the particles of high volatile compounds, while low volatile compounds will stay in the particle. This will lead to an overall decrease in volatility, as well as narrowing the volatility distribution. Although the OH exposure was found to be the major driver to reduced volatility in SAPHIR, it should also be noted, that the long time scales makes it possible for slower reactions to take place which can also lead to a further reduction in volatility.

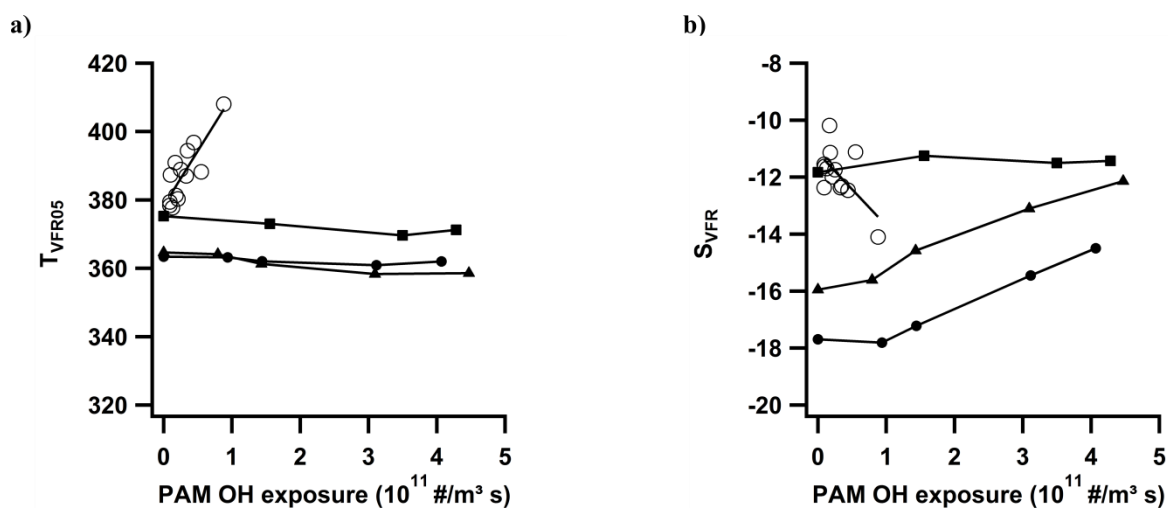


**Figure 5.7**  $T_{VFR0.5}$  (a) and  $S_{VFR}$  (b) plotted as functions of OH-exposure for  $\alpha$ -pinene (closed circles),  $\beta$ -pinene (closed triangles), limonene (closed squares) and for SAPHIR (open circles).

## 5.3 Production of secondary aerosol mass from exhaust emissions

As a part of this work a OFR, called Go:PAM, has been developed which enables studies of secondary particle formation from rapidly changing emissions source. Go:PAM was used to study formation of secondary particle mass of exhaust emissions from 29 in-use transit buses under real-world conditions (Paper V). In order to better interpret the data, a chemical kinetic model was developed. This model was used to derive the minimum OH exposure for each plume measurement.

### 5.3.1 Studying exhaust emissions with Go:PAM

Figure 5.8 displays an example of four consecutive bus plumes sampled through the Go:PAM, where CO<sub>2</sub> was measured before and particle mass after the Go:PAM. After the bus passed the sampling inlet, the particle background concentration was reached within minutes. This allows studies of rapid changing emission sources, and furthermore, the short refresh time enables studies of high number of bus individual in relative short time period.

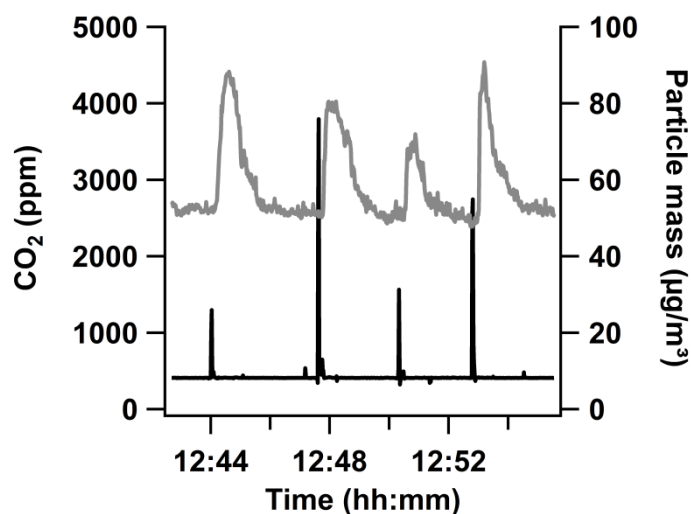


**Figure 5.8** Example of data from the bus measurements. The concentration of CO<sub>2</sub> (black line) was measured before the Go:PAM and the particle mass (grey line) after the Go:PAM.

For the standard set-up sampling ambient air without the emission plume, an OH-exposure of around  $5 \times 10^{11}$  molecules cm<sup>-3</sup> s was derived. This represents obviously the upper limit since the OH-exposure will be reduced by increased OH reactivity of compounds in the plumes and by NO titration of the OH precursor O<sub>3</sub>. So in order to better interpret the data, a simple chemical kinetic model was developed to estimate the minimum OH exposure in each plume. The model is based on kinetic data used by Peng et al (2015), with minor corrections and modifications to match the Go:PAM conditions. For every single passage, the maximum concentration of carbon monoxide (CO) and total emitted hydrocarbon



was estimated using the RSD data, and this was used to calculate the external OH reactivity. For the CNG buses, formaldehyde was used as a proxy for reactivity of the hydrocarbons [Karavalakis et al., 2016] and for RME and for the diesel buses toluene was used to represent the reactivity of the complex mixture [Montero et al., 2010]. Furthermore, the maximum plume concentration of NO was also estimated, and this was used to calculate the reduction in OH production due to the concentration decrease of O<sub>3</sub>. These plume maximums together with additional information about the absolute humidity, ozone concentration and residence time was used to model the minimum OH exposure for each plume. The modelled OH exposure varied from  $2.4 \times 10^9$  to  $2.2 \times 10^{12}$  molecules cm<sup>-3</sup> s. The modelled minimum OH exposure facilitates a more realistic interpretation of the secondary particle formation of plume emissions.

### 5.3.2 Secondary particle formation of emissions from in-use transit buses

Fresh and aged exhaust emissions from 29 individual buses running on diesel, CNG and RME were studied. 5 of the 11 RME buses were hybrid electric vehicles. In total 348 plumes were extracted and analyzed. From Figure 5.9 it can be seen that the primary particle emissions depend on the fuel. However, for the formation of secondary mass the picture is not as clear. The diesel buses had the highest median  $EF_{PM:aged}$ , and following in the descending order by RME, RME<sub>HEV</sub> and CNG. In parallel to this work, chemical analysis of the exhaust plumes found a large fraction (37-72%) of the identified compounds from all fuel types [Le Breton et al., 2017]. This indicates that there is an important non-fuel related source for the secondary particle formation, and one suggested source for this can be co-emissions of lubrication oil and/or fuel additives [Le Breton et al., 2017]. Furthermore, all fuel types were represented among the 5 buses forming the highest secondary mass at similar OH exposure, supporting a non-fuel dependent fuel source.

As can be seen from Figure 5.9, independent of fuel and technology, generally the secondary aerosol mass was much higher than the primary aerosol mass. For 79 % of the buses the average aged mass was 10 times higher than the fresh particle mass. The increase was largest for the RME and the CNG buses, with  $EF_{PM:Aged}$  with 53 and 50 times higher than  $EF_{PM:fresh}$ , respectively. This increase was smaller for the diesel (7) and the RME<sub>HEV</sub> (5) buses. However, it should be noted that in absolute numbers  $EF_{PM:Aged}$  was the largest for the diesel and RME buses.

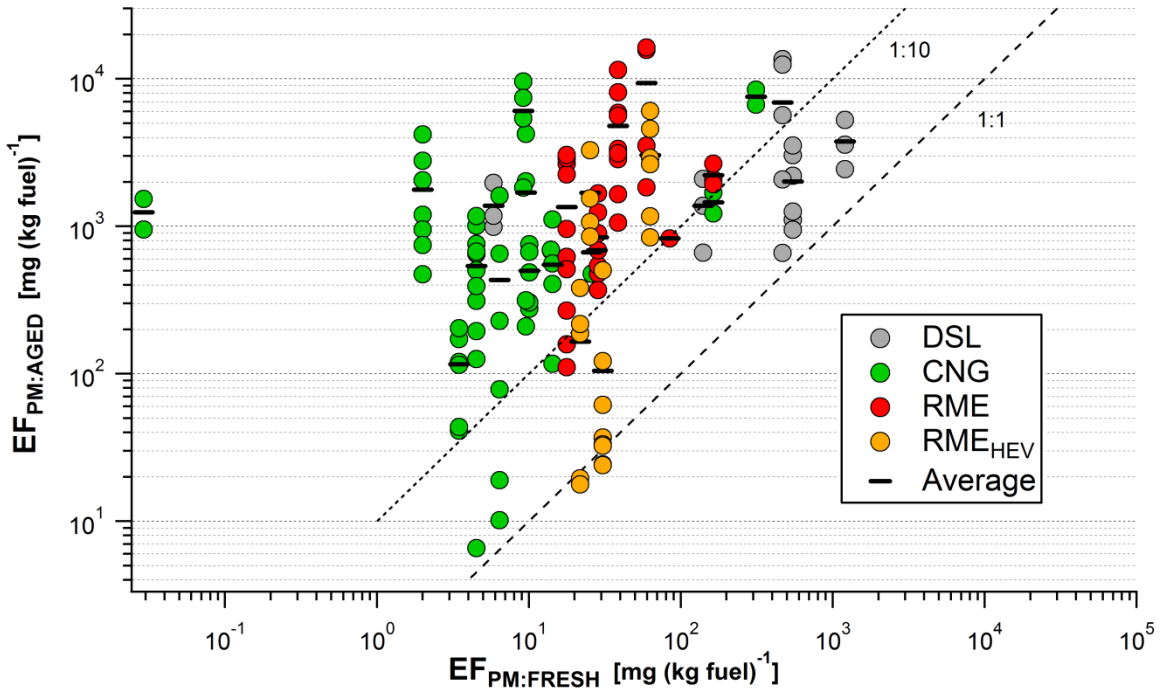


**Figure 5.9**  $EF_{PM:AGED}$  versus average  $EF_{PM:FRESH}$  for all the studied bus passages with respect to fuel type. Dashed lines are the 1:10 and 1:1 lines and solid lines are bus averages.

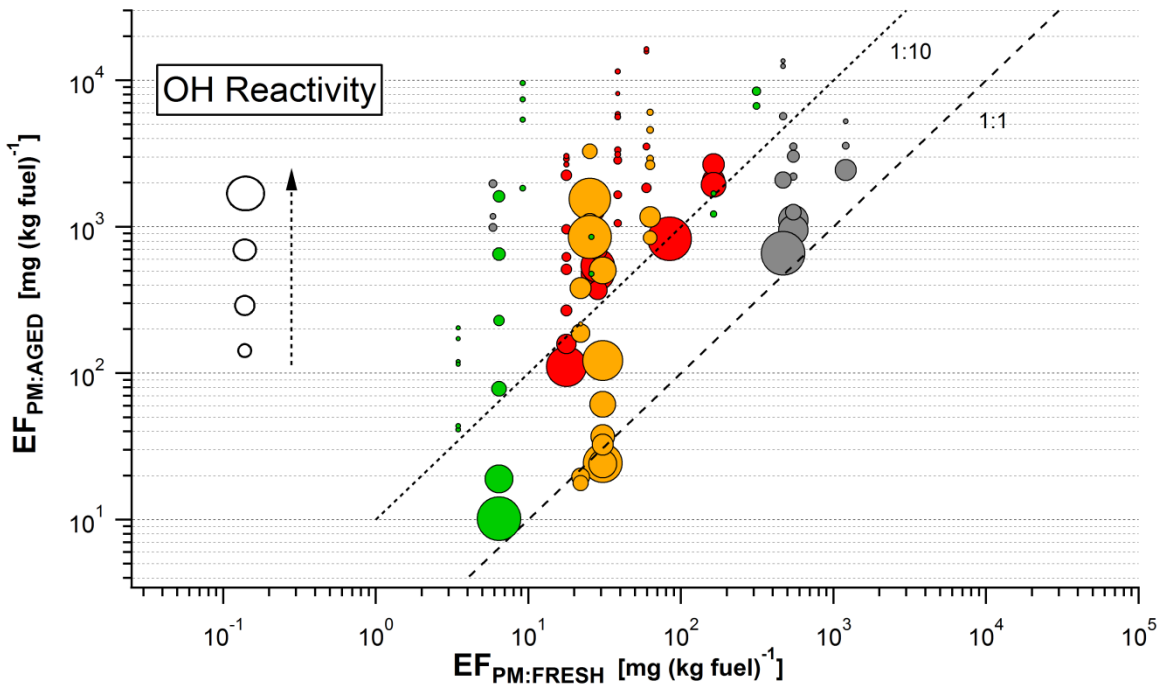


**Figure 5.10**  $EF_{PM:AGED}$  versus average  $EF_{PM:FRESH}$  for all the studied bus passages with respect to fuel type as a function of OH reactivity in the different fuel classes.

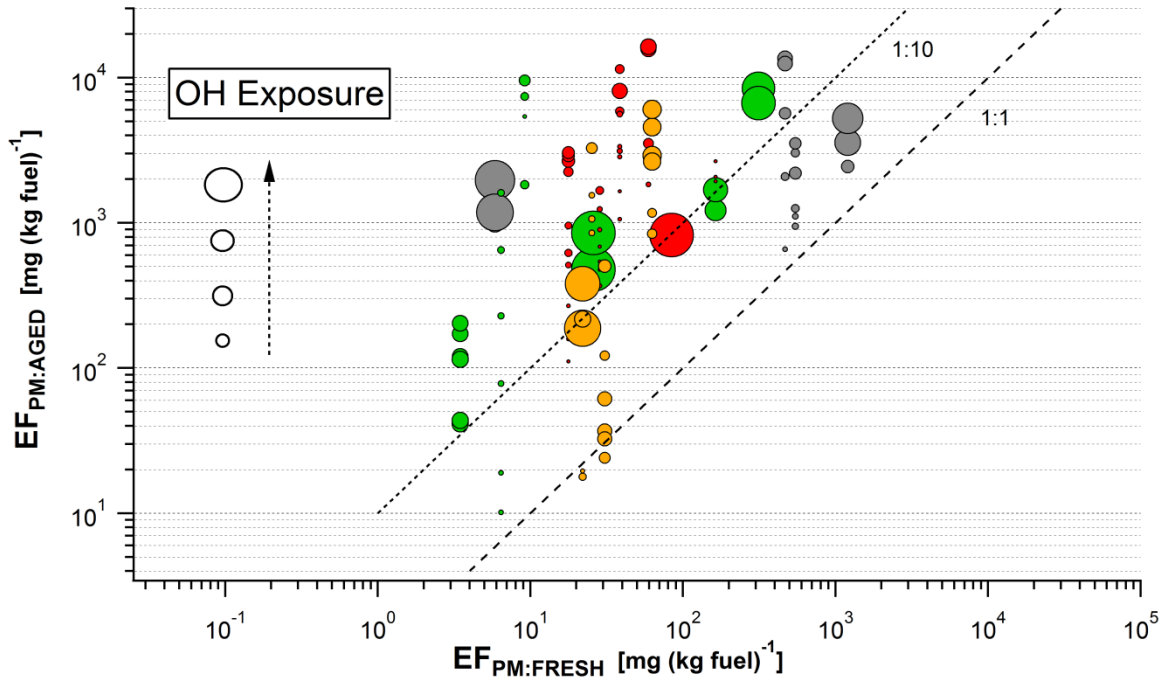


**Figure 5.11**  $EF_{PM:AGED}$  versus average  $EF_{PM:FRESH}$  for all the studied bus passages with respect to fuel type as a function of OH exposure (range:  $5.0 \times 10^{10}$  -  $1.48 \times 10^{12}$  (CNG  $2.17 \times 10^{12}$ ) molecules  $cm^{-3} s$ )

As shown in Figure 5.9, there is a significant variation in the secondary mass formed between the different passages of the same bus, and as illustrated in Figure 5.10, this variation depends primarily on the emitted compounds and their dilution before being sampled into Go:PAM. An increased OH reactivity will decrease the OH radicals available for oxidation of compounds which leads to a decrease in formation of secondary particles. Furthermore, Figure 5.11 shows the estimated minimum OH exposure for each plume, and as can be seen for RME, RME<sub>HEV</sub> and DSL buses most of the variation in the  $EF_{PM:Aged}$  can be explained by differences in the minimum OH exposure. For the CNG buses, on the other hand, the trend is less clear. This indicates that there are larger differences in the chemical composition of the emissions between the passages of the same CNG bus compared to the buses running on the other tested fuels. This is supported by larger variation in the gaseous emissions and primary particle emissions for CNG buses compared to RME and DSL. Furthermore, Figure 5.11 shows that there are some passages where there is a large production of secondary particle mass even at low minimum OH exposure. In these cases, there were supposedly high emissions of compounds more prone to form secondary aerosol mass in these passages. In summary, the results show quite clearly that the formation of secondary particles strongly depends on the OH exposure, and this indicates that in order to correctly interpret data from plume measurements it is a key to either measure or model the actual OH in the OFR for each plume.

## 6. Atmospheric implications

A key question needed to be discussed in order to understand and interpret the atmospheric implications of this work is: What does laboratory studies of secondary aerosols tell us about the aerosols in the ambient atmosphere? Laboratory studies are an essential link between ambient measurements and modelling of the atmosphere [Burkholder et al., 2017], and therefore a key needed when designing air quality strategies and predicting the climate forcing of SOA.

This work shows that freshly formed monoterpene SOA comprise compounds with a wide distribution of volatilities ranging from semi volatile compounds to compounds with extremely low volatility. Monoterpene oxidation products will therefore in the atmosphere contribute both to the formation of new particles and to particle growth by condensation, and this demonstrates the importance of including parametrization of monoterpene oxidation in order to predict the climate forcing of SOA.

The detailed laboratory studies on the atmospheric monoterpene oxidation give insight on how this SOA formation can be parametrized. The combined results from Paper I-II emphasize the impact of the chemical structure of monoterpenes on their efficiency to produce secondary organic aerosols (SOA) and on the thermal properties of the aerosols formed. First of all, there is a striking difference in formation of SOA from limonene compared to  $\alpha$ -pinene. This, together with recent findings on production of compounds with extremely low volatility from the ozonolysis of limonene [Ehn et al., 2014; Jokinen et al., 2015; Mentel et al., 2015], calls for incorporation of limonene oxidation in the parameterization of SOA formation. Whereas it is of high priority to incorporate limonene parameterization, the results in this work indicate that at this stage it is of less importance to include parameterization of SOA formation from  $\beta$ -pinene oxidation. The results, combined with relatively low atmospheric concentration of  $\beta$ -pinene compared to  $\alpha$ -pinene [Hakola et al., 2012] and the slow reaction rate of  $\beta$ -pinene with ozone [Atkinson and Arey, 2003], justify not prioritizing this parameterization. However, it should be kept in mind that the differences in response for endo- and exo-cyclic monoterpenes would make any inclusion of the SOA parameterization more realistic, and could improve the prediction of the climate forcing of SOA.

Atmospheric aging of SOA can be studied both in atmospheric simulation chambers and oxidation flow reactors (OFR), and comparison to ambient measurements have shown that both systems can produce aerosols with typical real atmosphere characteristics [Bruns et al., 2015; Chhabra et al., 2015; Kang et al., 2011; Ortega et al., 2016]. The present work, however, reveals that there are important differences between the two systems influencing the evolution of thermal properties. In the two systems, different processes drives this evolution: In larger atmospheric simulation chambers, such as

SAPHIR, there is a successive dilution of the sample which together with increased OH exposure leads to a reduction in particle volatility as the aerosol is aged. In OFRs, on the other hand, an increased OH exposure will lead to faster oxidation and enhanced particle mass production. This will lead to more semi volatile compounds partitioning towards the condensed phase, and at the same time, higher OH exposure also leads to secondary oxidation providing lower volatility products. Together, this will broaden the volatility distribution of the compounds in the particles. In the atmosphere, however, there will both be successive dilution of the aerosol and an inflow of fresh material. As an example, imagine an air parcel which moves from an atmosphere influenced by biogenic emissions to an urban atmosphere. Above the canopy there will be successive dilution of the biogenic compounds, but as the air parcel is transported towards an urban environment there will also be an enhanced inflow of fresh anthropogenic emissions. Therefore, to understand formation and aging of secondary aerosols in the atmosphere, data from both flow reactors and chambers are needed.

Formation and aging of secondary aerosols also affect people's health directly by influencing the air quality in urban areas. There can be a significant formation of secondary aerosols from traffic-related emission sources [Gentner et al., 2017], and the contribution of air pollutants from heavy duty vehicles (HDV) is often substantial [Enroth et al., 2016]. Therefore the choice of fuel and technology of HDV, including transit buses, can affect the quality of life for a considerably number of people. In this work, it was found for in-use transit buses under real-life driving conditions that the secondary particulate mass was 10 times higher than the primary particle emissions. Although in this work only emissions from transit buses were studied, the secondary particle formation from other vehicle categories and emission sources (e.g. shipping and industry) that influence urban areas should also be investigated. This result calls for the consideration of the secondary particle formation when evaluating the environmental impact of different emission sources.

To conclude, this work highlights the importance of understanding formation and aging of secondary aerosols in order to ensure high quality of life for as many as possible. The results provide insight into processes that are important for a more accurate prediction of the climate forcing of SOA. Furthermore, the results emphasize the importance of including secondary particle formation when designing air quality strategies.

# Acknowledgements

*"I think you learn much more if you have fun."* Nobel Laureate May Britt Moser

Being a PhD student is a lot of blood, sweat and tears. And fun. Mostly fun! There are many that have contributed to this time being a great experience. Firstly, I would like to thank my supervisor, Professor Mattias Hallquist, who gave me the opportunity to carry out this research. Thanks for always supporting me and giving me space for trial and error. That has been important for my development as a scientist. I respect your efforts to make the world a better place! Secondly, Emeritus Professor Evert Ljungström is acknowledged not only for being my examiner the first years, but for the valued help and support in the lab, especially with Go:PAM, and for always having the time for me. I appreciate that your endless patience when discussing all my questions. I will also like to thank, Professor Johan Boman, who guided me in finalizing my thesis, always asking me the right questions at the right time, even the questions that I did not want to get.

I have been included in many interesting projects during my time as PhD student. Dr. Åsa Hallquist, thanks for including me in your projects. I really enjoy working with you! I would also like to thank Dr Thomas Mentel, who gave me the opportunity to visit and work at SAPHIR. I'm still thankful for the coffee you provided us with on the weekends. Dr. Kasper Kristensen and Professor Marianne Glasius are acknowledged for introducing me for the world of dimer esters, filter sampling and long abbreviations. The research presented is a contribution to the Swedish strategic research areas Transport and MERGE (Modelling the Regional and Global Earth system). I would acknowledge the funders for respectively paper and especially the financial support from: Vinnova, Sweden's Innovation Agency under contract 2013-03058, Formas (grant number 214-2013-1430, 214-2010-1756), the Swedish Research Council (grant number 2014-05332 and 80475101) and the Swedish EPA research programme CLEO.

Being a PhD student is not only research. Dr. Erik Thomson, thanks always taking the time whenever I needed advice on science, life, bikes, försäkringskassan and all other kinds of things. Associate Professor Marie Thynell, thank you for taking the time in your extremely busy schedule and share from your experience. Dr. Jenny Mattson is acknowledged for inspiring discussions on text, language and writing.

There is also a lot of practical things that has to be solved as PhD student, and I have met many helpful people long my way: Benny Lönn is acknowledged for skillful work with the Go:PAM and Maria Liritsi for always opening doors for me. I would also like to thank Henrik and Martin at IVL. Västtrafik, the bus drivers and the personnel at the measurement sites are gratefully acknowledged for their assistance and hospitality.

As a PhD student I have met many Swedes, Danes, Finns, Russians, Chinese, Germans, Austrians, Swiss and Americans who all have made this much richer experience. Especially thanks to Anna, my SOA soulmate, I have learnt so much from discussing with you! (Not only about science...) Also thanks to Eva, for introducing me to the mysteries of G-FROST, Jonathan, for exploring with the PAM chamber with me (and the early lunches), Kong, for being a great office mate, Sam, for searching for the flow together. Julia H. and Sofia J., for sismance, Mike, for your support on bus issues, Dan, for the productive sessions, Pei, for all technical support, Camilla, for taking good care of me when teaching, Jennie, for sharing the same passion for jympa, science and justice, Susana and Nönne, for being inspiring, but also for being honest about what it takes to survive in science. Thanks to current and former members of the atmospheric science group creating a good environment, both for scientific work and for me to be me.

Ikkje minst, takk til Samuel, mitt faste haldepunkt, min viktigaste støttespeler og min beste ven! Og til Eldar og Sindre, som kvar dag minner meg på at det er andre viktige ting i livet enn eksperiment, artiklar og undervisning. Eg håper eg har bidratt til å gjere lufta litt betre for dåke!

# References

- Alanen J, Simonen P, Saarikoski S, Timonen H, Kangasniemi O, Saukko E, Hillamo R, Lehtoranta K, Murtonen T, Vesala H, Keskinen J, Ronkko T: Comparison of primary and secondary particle formation from natural gas engine exhaust and of their volatility characteristics. *Atmospheric Chemistry and Physics* 2017;17:8739-8755.
- Atkinson R, Arey J: Gas-phase tropospheric chemistry of biogenic volatile organic compounds: a review. *Atmospheric Environment* 2003;37:197-219.
- Berndt T, Richters S, Jokinen T, Hyttinen N, Kurten T, Otkjaer RV, Kjaergaard HG, Stratmann F, Herrmann H, Sipila M, Kulmala M, Ehn M: Hydroxyl radical-induced formation of highly oxidized organic compounds. *Nat Commun* 2016;7:13677.
- Bruns EA, El Haddad I, Keller A, Klein F, Kumar K, Pieber SM, Corbin JC, Slowik JG, Brune WH, Baltensperger U, Prévôt ASH: Inter-comparison of laboratory smog chamber and flow reactor systems on organic aerosol yield and composition. *Atmospheric Measurement Techniques* 2015;8:2315-2332.
- Burkholder JB, Abbatt JP, Barnes I, Roberts JM, Melamed ML, Ammann M, Bertram AK, Cappa CD, Carlton AG, Carpenter LJ, Crowley JN, Dubowski Y, George C, Heard DE, Herrmann H, Keutsch FN, Kroll JH, McNeill VF, Ng NL, Nizkorodov SA, Orlando JJ, Percival CJ, Picquet-Varrault B, Rudich Y, Seakins PW, Surratt JD, Tanimoto H, Thornton JA, Tong Z, Tyndall GS, Wahner A, Weschler CJ, Wilson KR, Ziemann PJ: The Essential Role for Laboratory Studies in Atmospheric Chemistry. *Environ Sci Technol* 2017;51:2519-2528.
- Cappa CD, Wilson KR: Evolution of organic aerosol mass spectra upon heating: implications for OA phase and partitioning behavior. *Atmospheric Chemistry and Physics* 2011;11:1895-1911.
- Cassee FR, Héroux M-E, Gerlofs-Nijland ME, Kelly FJ: Particulate matter beyond mass: recent health evidence on the role of fractions, chemical constituents and sources of emission. *Inhalation Toxicology* 2013;25:802-812.
- Chhabra PS, Lambe AT, Canagaratna MR, Stark H, Jayne JT, Onasch TB, Davidovits P, Kimmel JR, Worsnop DR: Application of high-resolution time-of-flight chemical ionization mass spectrometry measurements to estimate volatility distributions of  $\alpha$ -pinene and naphthalene oxidation products. *Atmospheric Measurement Techniques* 2015;8:1-18.
- Cohen AJ, Brauer M, Burnett R, Anderson HR, Frostad J, Estep K, Balakrishnan K, Brunekreef B, Dandona L, Dandona R, Feigin V, Freedman G, Hubbell B, Jobling A, Kan H, Knibbs L, Liu Y, Martin R, Morawska L, Pope CA, Shin H, Straif K, Shaddick G, Thomas M, van Dingenen R, van Donkelaar A, Vos T, Murray CJL, Forouzanfar MH: Estimates and 25-year trends of the global burden of disease attributable to ambient air pollution: an analysis of data from the Global Burden of Diseases Study 2015. *The Lancet* 2017;389:1907-1918.
- Dallmann TR, Onasch TB, Kirchstetter TW, Worton DR, Fortner EC, Herndon SC, Wood EC, Franklin JP, Worsnop DR, Goldstein AH, Harley RA: Characterization of particulate matter emissions from on-road gasoline and diesel vehicles using a soot particle aerosol mass spectrometer. *Atmospheric Chemistry and Physics* 2014;14:7585-7599.
- Donahue NM, Epstein SA, Pandis SN, Robinson AL: A two-dimensional volatility basis set: 1. organic-aerosol mixing thermodynamics. *Atmospheric Chemistry and Physics* 2011;11:3303-3318.
- Donahue NM, Henry KM, Mentel TF, Kiendler-Scharr A, Spindler C, Bohn B, Brauers T, Dorn HP, Fuchs H, Tillmann R, Wahner A, Saathoff H, Naumann KH, Mohler O, Leisner T, Müller L, Reinnig MC, Hoffmann T, Salo K, Hallquist M, Frosch M, Bilde M, Tritscher T, Barmet P, Praplan AP, DeCarlo PF, Dommen J, Prevot AS, Baltensperger U: Aging of biogenic secondary organic aerosol via gas-phase OH radical reactions. *Proc Natl Acad Sci U S A* 2012;109:13503-13508.
- Drozd GT, Kroll J, Donahue NM: 2,3-Dimethyl-2-butene (TME) Ozonolysis: Pressure Dependence of Stabilized Criegee Intermediates and Evidence of Stabilized Vinyl Hydroperoxides. *The Journal of Physical Chemistry A* 2011;115:161-166.
- Dunmore RE, Hopkins JR, Lidster RT, Lee JD, Evans MJ, Rickard AR, Lewis AC, Hamilton JF: Diesel-related hydrocarbons can dominate gas phase reactive carbon in megacities. *Atmos Chem Phys* 2015;15:9983-9996.
- Edwards R, Larive J-F, Rickeard D, Weindorf W: WELL-TO-WHEELS ANALYSIS OF FUTURE AUTOMOTIVE FUELS AND POWERTRAINS IN THE EUROPEAN CONTEXT. European Commission, Joint Research Centre 2014.

- Ehn M, Thornton JA, Kleist E, Sipila M, Junninen H, Pullinen I, Springer M, Rubach F, Tillmann R, Lee B, Lopez-Hilfiker F, Andres S, Acir IH, Rissanen M, Jokinen T, Schobesberger S, Kangasluoma J, Kontkanen J, Nieminen T, Kurten T, Nielsen LB, Jorgensen S, Kjaergaard HG, Canagaratna M, Maso MD, Berndt T, Petaja T, Wahner A, Kerminen VM, Kulmala M, Worsnop DR, Wildt J, Mentel TF: A large source of low-volatility secondary organic aerosol. *Nature* 2014;506:476-479.
- Enroth J, Saarikoski S, Niemi J, Kousa A, Jezek I, Mocnik G, Carbone S, Kuuluvainen H, Ronkko T, Hillamo R, Pirjola L: Chemical and physical characterization of traffic particles in four different highway environments in the Helsinki metropolitan area. *Atmospheric Chemistry and Physics* 2016;16:5497-5512.
- Finlayson-Pitts BJ, Pitts Jr JN: Preface; in: *Chemistry of the Upper and Lower Atmosphere*. San Diego, Academic Press, 2000, pp xvii-xviii.
- Friedman B, Link MF, Fulgham SR, Brophy P, Galang A, Brune WH, Jathar SH, Farmer DK: Primary and Secondary Sources of Gas-Phase Organic Acids from Diesel Exhaust. *Environ Sci Technol* 2017;51:10872-10880.
- Gentner DR, Jathar SH, Gordon TD, Bahreini R, Day DA, El Haddad I, Hayes PL, Pieber SM, Platt SM, de Gouw J, Goldstein AH, Harley RA, Jimenez JL, Prevot AS, Robinson AL: Review of Urban Secondary Organic Aerosol Formation from Gasoline and Diesel Motor Vehicle Emissions. *Environ Sci Technol* 2017;51:1074-1093.
- Glasius M, Goldstein AH: Recent Discoveries and Future Challenges in Atmospheric Organic Chemistry. *Environmental Science & Technology* 2016;50:2754-2764.
- Goldstein AH, Galbally IE: Known and Unexplored Organic Constituents in the Earth's Atmosphere. *Environmental Science & Technology* 2007;41:1514-1521.
- Gordon TD, Presto AA, May AA, Nguyen NT, Lipsky EM, Donahue NM, Gutierrez A, Zhang M, Maddox C, Rieger P, Chattopadhyay S, Maldonado H, Maricq MM, Robinson AL: Secondary organic aerosol formation exceeds primary particulate matter emissions for light-duty gasoline vehicles. *Atmospheric Chemistry and Physics* 2014a;14:4661-4678.
- Gordon TD, Presto AA, Nguyen NT, Robertson WH, Na K, Sahay KN, Zhang M, Maddox C, Rieger P, Chattopadhyay S, Maldonado H, Maricq MM, Robinson AL: Secondary organic aerosol production from diesel vehicle exhaust: impact of aftertreatment, fuel chemistry and driving cycle. *Atmos Chem Phys* 2014b;14:4643-4659.
- Grigoratos T, Martini G: Non-exhaust traffic related emissions. Brake and tyre wear PM. *JRC Science and Policy Reports* 2014.
- Guenther AB, Jiang X, Heald CL, Sakulyanontvittaya T, Duhl T, Emmons LK, Wang X: The Model of Emissions of Gases and Aerosols from Nature version 2.1 (MEGAN2.1): an extended and updated framework for modeling biogenic emissions. *Geoscientific Model Development* 2012;5:1471-1492.
- Hakola H, Hellén H, Hemmilä M, Rinne J, Kulmala M: In situ measurements of volatile organic compounds in a boreal forest. *Atmos Chem Phys* 2012;12:11665-11678.
- Hakola H, Patokoski J, Hellén H, Tarvainen T, Rinne J: Annual variations of atmospheric VOC concentrations in a boreal forest. *BOREAL ENVIRONMENT RESEARCH* 2009;14:722-730.
- Hallquist M, Wenger JC, Baltensperger U, Rudich Y, Simpson D, Claeys M, Dommen J, Donahue NM, George C, Goldstein AH, Hamilton JF, Herrmann H, Hoffmann T, Iinuma Y, Jang M, Jenkin ME, Jimenez JL, Kiendler-Scharr A, Maenhaut W, McFiggans G, Mentel TF, Monod A, Prévôt ASH, Seinfeld JH, Surratt JD, Szmigielski R, Wildt J: The formation, properties and impact of secondary organic aerosol: current and emerging issues. *Atmos Chem Phys* 2009;9:5155-5236.
- Hallquist ÅM, Jerksjö M, Fallgren H, Westerlund J, Sjödin Å: Particle and gaseous emissions from individual diesel and CNG buses. *Atmospheric Chemistry and Physics* 2013;13:5337-5350.
- Hohaus T, Gensch I, Kimmel J, Worsnop D, Kiendler-Scharr A: Experimental determination of the partitioning coefficient of  $\beta$ -pinene oxidation products in SOA. *Physical Chemistry Chemical Physics* 2015;17:14796-14804.
- Jathar SH, Friedman B, Galang AA, Link MF, Brophy P, Volckens J, Eluri S, Farmer DK: Linking Load, Fuel, and Emission Controls to Photochemical Production of Secondary Organic Aerosol from a Diesel Engine. *Environmental Science & Technology* 2017;51:1377-1386.
- Jimenez JL, Canagaratna MR, Donahue NM, Prevot AS, Zhang Q, Kroll JH, DeCarlo PF, Allan JD, Coe H, Ng NL, Aiken AC, Docherty KS, Ulbrich IM, Grieshop AP, Robinson AL, Duplissy J, Smith JD, Wilson KR, Lanz VA, Hueglin C, Sun YL, Tian J, Laaksonen A, Raatikainen T, Rautiainen J, Vaattovaara P, Ehn M, Kulmala M, Tomlinson JM, Collins DR, Cubison MJ, Dunlea EJ, Huffman JA, Onasch TB, Alfarra MR, Williams PI, Bower K, Kondo Y, Schneider J, Drewnick F, Borrmann S, Weimer S, Demerjian K, Salcedo D, Cottrell L, Griffin R, Takami A, Miyoshi T, Hatakeyama S, Shimono A, Sun JY, Zhang YM, Dzepina K, Kimmel JR,



- Sueper D, Jayne JT, Herndon SC, Trimborn AM, Williams LR, Wood EC, Middlebrook AM, Kolb CE, Baltensperger U, Worsnop DR: Evolution of organic aerosols in the atmosphere. *Science* 2009;326:1525-1529.
- Jokinen T, Berndt T, Makkonen R, Kerminen VM, Junninen H, Paasonen P, Stratmann F, Herrmann H, Guenther AB, Worsnop DR, Kulmala M, Ehn M, Sipila M: Production of extremely low volatile organic compounds from biogenic emissions: Measured yields and atmospheric implications. *Proc Natl Acad Sci U S A* 2015;112:7123-7128.
- Jonsson ÅM, Hallquist M, Ljungström E: The effect of temperature and water on secondary organic aerosol formation from ozonolysis of limonene,  $\Delta^3$ -carene and  $\alpha$ -pinene. *Atmos Chem Phys* 2008a;8:6541-6549.
- Jonsson ÅM, Hallquist M, Ljungström E: Influence of OH Scavenger on the Water Effect on Secondary Organic Aerosol Formation from Ozonolysis of Limonene,  $\Delta^3$ -Carene, and  $\alpha$ -Pinene. *Environmental Science & Technology* 2008b;42:5938-5944.
- Jonsson ÅM, Hallquist M, Saathoff H: Volatility of secondary organic aerosols from the ozone initiated oxidation of  $\alpha$ -pinene and limonene. *Journal of Aerosol Science* 2007;38:843-852.
- Kanakidou M, Seinfeld JH, Pandis SN, Barnes I, Dentener FJ, Facchini MC, Van Dingenen R, Ervens B, Nenes A, Nielsen CJ, Swietlicki E, Putaud JP, Balkanski Y, Fuzzi S, Horth J, Moortgat GK, Winterhalter R, Myhre CEL, Tsigaridis K, Vignati E, Stephanou EG, Wilson J: Organic aerosol and global climate modelling: a review. *Atmos Chem Phys* 2005;5:1053-1123.
- Kang E, Root MJ, Toohey DW, Brune WH: Introducing the concept of Potential Aerosol Mass (PAM). *Atmos Chem Phys* 2007;7:5727-5744.
- Kang E, Toohey DW, Brune WH: Dependence of SOA oxidation on organic aerosol mass concentration and OH exposure: experimental PAM chamber studies. *Atmospheric Chemistry and Physics* 2011;11:1837-1852.
- Karavalakis G, Hajbabaie M, Jiang Y, Yang J, Johnson KC, Cocker DR, Durbin TD: Regulated, greenhouse gas, and particulate emissions from lean-burn and stoichiometric natural gas heavy-duty vehicles on different fuel compositions. *Fuel* 2016;175:146-156.
- Karjalainen P, Timonen H, Saukko E, Kuuluvainen H, Saarikoski S, Aakko-Saksa P, Murtonen T, Bloss M, Dal Maso M, Simonen P, Ahlberg E, Svenningsson B, Brune WH, Hillamo R, Keskinen J, Ronkko T: Time-resolved characterization of primary particle emissions and secondary particle formation from a modern gasoline passenger car. *Atmospheric Chemistry and Physics* 2016a;16:8559-8570.
- Karjalainen P, Timonen H, Saukko E, Kuuluvainen H, Saarikoski S, Aakko-Saksa P, Murtonen T, Bloss M, Dal Maso M, Simonen P, Ahlberg E, Svenningsson B, Brune WH, Hillamo R, Keskinen J, Rönkkö T: Time-resolved characterization of primary particle emissions and secondary particle formation from a modern gasoline passenger car. *Atmospheric Chemistry and Physics* 2016b;16:8559-8570.
- Khamaganov V, Hites RA: Rate Constants for the Gas-Phase Reactions of Ozone with Isoprene,  $r$ - and  $\alpha$ -Pinene, and Limonene as a Function of Temperature. *Journal of Physical Chemistry A* 2001;105:815-822.
- Kolesar KR, Li Z, Wilson KR, Cappa CD: Heating-Induced Evaporation of Nine Different Secondary Organic Aerosol Types. *Environ Sci Technol* 2015;49:12242-12252.
- Kourtchev I, Giorio C, Manninen A, Wilson E, Mahon B, Aalto J, Kajos M, Venables D, Ruuskanen T, Levula J, Loponen M, Connors S, Harris N, Zhao D, Kiendler-Scharr A, Mentel T, Rudich Y, Hallquist M, Doussin JF, Maenhaut W, Back J, Petaja T, Wenger J, Kulmala M, Kalberer M: Enhanced Volatile Organic Compounds emissions and organic aerosol mass increase the oligomer content of atmospheric aerosols. *Sci Rep* 2016;6:35038.
- Kristensen K, Bilde M, Aalto PP, Petäjä T, Glasius M: Denuder/filter sampling of organic acids and organosulfates at urban and boreal forest sites: Gas/particle distribution and possible sampling artifacts. *Atmospheric Environment* 2016;130:36-53.
- Kristensen K, Cui T, Zhang H, Gold A, Glasius M, Surratt JD: Dimers in  $\alpha$ -pinene secondary organic aerosol: effect of hydroxyl radical, ozone, relative humidity and aerosol acidity. *Atmospheric Chemistry and Physics* 2014;14:4201-4218.
- Kristensen K, Enggrob KL, King SM, Worton DR, Platt SM, Mortensen R, Rosenoern T, Surratt JD, Bilde M, Goldstein AH, Glasius M: Formation and occurrence of dimer esters of pinene oxidation products in atmospheric aerosols. *Atmospheric Chemistry and Physics* 2013;13:3763-3776.
- Lambe AT, Ahern AT, Williams LR, Slowik JG, Wong JPS, Abbatt JPD, Brune WH, Ng NL, Wright JP, Croasdale DR, Worsnop DR, Davidovits P, Onasch TB: Characterization of aerosol photooxidation flow reactors: heterogeneous oxidation, secondary organic aerosol formation and cloud condensation nuclei activity measurements. *Atmospheric Measurement Techniques* 2011;4:445-461.

- Laothawornkitkul J, Taylor JE, Paul ND, Hewitt CN: Biogenic volatile organic compounds in the Earth system. *New Phytol* 2009;183:27-51.
- Le Breton M, Psichoudaki M, Hallquist M, Watne ÅK, Hallquist ÅM: Utilization of FIGAERO ToF-CIMS for evaluation of fresh and aged particulate emissions from diesel, CNG and RME fueled buses. Submitted to *Environmental Science and Technology* 2017.
- Lee B-H, Pierce JR, Engelhart GJ, Pandis SN: Volatility of secondary organic aerosol from the ozonolysis of monoterpenes. *Atmospheric Environment* 2011;45:2443-2452.
- Lough GC, Schauer JJ, Park J-S, Shafer MM, DeMinter JT, Weinstein JP: Emissions of Metals Associated with Motor Vehicle Roadways. *Environmental Science & Technology* 2005;39:826-836.
- Maher BA, Ahmed IA, Karloukovski V, MacLaren DA, Foulds PG, Allsop D, Mann DM, Torres-Jardon R, Calderon-Garciduenas L: Magnetite pollution nanoparticles in the human brain. *Proc Natl Acad Sci U S A* 2016;113:10797-10801.
- Matti Maricq M: Chemical characterization of particulate emissions from diesel engines: A review. *Journal of Aerosol Science* 2007;38:1079-1118.
- Mentel TF, Springer M, Ehn M, Kleist E, Pullinen I, Kurtén T, Rissanen M, Wahner A, Wildt J: Formation of highly oxidized multifunctional compounds: autoxidation of peroxy radicals formed in the ozonolysis of alkenes – deduced from structure–product relationships. *Atmospheric Chemistry and Physics* 2015;15:6745-6765.
- Mohr C, Lopez-Hilfiker FD, Yli-Juuti T, Heitto A, Lutz A, Hallquist M, D'Ambro EL, Rissanen MP, Hao L, Schobesberger S, Kulmala M, Mauldin RL, Makkonen U, Sipilä M, Petäjä T, Thornton JA: Ambient observations of dimers from terpene oxidation in the gas phase: Implications for new particle formation and growth. *Geophysical Research Letters* 2017;44:2958-2966.
- Montero L, Duane M, Manfredi U, Astorga C, Martini G, Carriero M, Krasenbrink A, Larsen BR: Hydrocarbon emission fingerprints from contemporary vehicle/engine technologies with conventional and new fuels. *Atmospheric Environment* 2010;44:2167-2175.
- Nguyen TL, Peeters J, Vereecken L: Theoretical study of the gas-phase ozonolysis of  $\beta$ -pinene (C<sub>10</sub>H<sub>16</sub>). *Physical Chemistry Chemical Physics* 2009;11:5643.
- Orlando JJ, Tyndall GS: Laboratory studies of organic peroxy radical chemistry: an overview with emphasis on recent issues of atmospheric significance. *Chem Soc Rev* 2012;41:6294-6317.
- Ortega AM, Hayes PL, Peng Z, Palm BB, Hu W, Day DA, Li R, Cubison MJ, Brune WH, Graus M, Warneke C, Gilman JB, Kuster WC, de Gouw J, Gutiérrez-Montes C, Jimenez JL: Real-time measurements of secondary organic aerosol formation and aging from ambient air in an oxidation flow reactor in the Los Angeles area. *Atmos Chem Phys* 2016;16:7411-7433.
- Ots R, Young DE, Vieno M, Xu L, Dunmore RE, Allan JD, Coe H, Williams LR, Herndon SC, Ng NL, Hamilton JF, Bergstrom R, Di Marco C, Nemitz E, Mackenzie IA, Kuenen JJP, Green DC, Reis S, Heal MR: Simulating secondary organic aerosol from missing diesel-related intermediate-volatility organic compound emissions during the Clean Air for London (ClearLo) campaign. *Atmospheric Chemistry and Physics* 2016;16:6453-6473.
- Palm BB, Campuzano-Jost P, Ortega AM, Day DA, Kaser L, Jud W, Karl T, Hansel A, Hunter JF, Cross ES, Kroll JH, Peng Z, Brune WH, Jimenez JL: In situ secondary organic aerosol formation from ambient pine forest air using an oxidation flow reactor. *Atmospheric Chemistry and Physics* 2016;16:2943-2970.
- Pankow JF: An absorption model of the gas/aerosol partitioning involved in the formation of secondary organic aerosol. *Atmospheric Environment* 1994;28:189-193.
- Pirjola L, Dittrich A, Niemi JV, Saarikoski S, Timonen H, Kuuluvainen H, Jarvinen A, Kousa A, Ronkko T, Hillamo R: Physical and Chemical Characterization of Real-World Particle Number and Mass Emissions from City Buses in Finland. *Environmental Science & Technology* 2016;50:294-304.
- Pirjola L, Rönkkö T, Saukko E, Parviainen H, Malinen A, Alanen J, Saveljef H: Exhaust emissions of non-road mobile machine: Real-world and laboratory studies with diesel and HVO fuels. *Fuel* 2017;202:154-164.
- Platt SM, El Haddad I, Zardini AA, Clairotte M, Astorga C, Wolf R, Slowik JG, Temime-Roussel B, Marchand N, Ježek I, Drinovec L, Močnik G, Möhler O, Richter R, Barmet P, Bianchi F, Baltensperger U, Prévôt ASH: Secondary organic aerosol formation from gasoline vehicle emissions in a new mobile environmental reaction chamber. *Atmospheric Chemistry and Physics* 2013;13:9141-9158.
- Pourkhesalian AM, Stevanovic S, Salimi F, Rahman MM, Wang H, Pham PX, Bottle SE, Masri AR, Brown RJ, Ristovski ZD: Influence of fuel molecular structure on the volatility and oxidative potential of biodiesel particulate matter. *Environ Sci Technol* 2014;48:12577-12585.

- Salo K, Hallquist M, Jonsson ÅM, Saathoff H, Naumann KH, Spindler C, Tillmann R, Fuchs H, Bohn B, Rubach F, Mentel TF, Müller L, Reinnig M, Hoffmann T, Donahue NM: Volatility of secondary organic aerosol during OH radical induced ageing. *Atmospheric Chemistry and Physics* 2011;11:11055-11067.
- Salo K, Jonsson ÅM, Andersson PU, Hallquist M: Aerosol Volatility and Enthalpy of Sublimation of Carboxylic Acids. *The Journal of Physical Chemistry A* 2010;114:4586-4594.
- Sato K, Jia T, Tanabe K, Morino Y, Kajii Y, Imamura T: Terpenylic acid and nine-carbon multifunctional compounds formed during the aging of  $\beta$ -pinene ozonolysis secondary organic aerosol. *Atmospheric Environment* 2016;130:127-135.
- Seco R, Peñuelas J, Filella I, Llusà J, Molowny-Horas R, Schallhart S, Metzger A, Müller M, Hansel A: Contrasting winter and summer VOC mixing ratios at a forest site in the Western Mediterranean Basin: the effect of local biogenic emissions. *Atmos Chem Phys* 2011;11:13161-13179.
- Shiraiwa M, Ueda K, Pozzer A, Lammel G, Kampf CJ, Fushimi A, Enami S, Arangio AM, Frohlich-Nowoisky J, Fujitani Y, Furuyama A, Lakey PSJ, Lelieveld J, Lucas K, Morino Y, Poschl U, Takahama S, Takami A, Tong H, Weber B, Yoshino A, Sato K: Aerosol health effects from molecular to global scales. *Environ Sci Technol* 2017.
- Shrivastava M, Cappa CD, Fan J, Goldstein AH, Guenther AB, Jimenez JL, Kuang C, Laskin A, Martin ST, Ng NL, Petaja T, Pierce JR, Rasch PJ, Roldin P, Seinfeld JH, Shilling J, Smith JN, Thornton JA, Volkamer R, Wang J, Worsnop DR, Zaveri RA, Zelenyuk A, Zhang Q: Recent advances in understanding secondary organic aerosol: Implications for global climate forcing. *Reviews of Geophysics* 2017;55:509-559.
- Shrivastava M, Easter RC, Liu X, Zelenyuk A, Singh B, Zhang K, Ma P-L, Chand D, Ghan S, Jimenez JL, Zhang Q, Fast J, Rasch PJ, Tiitta P: Global transformation and fate of SOA: Implications of low-volatility SOA and gas-phase fragmentation reactions. *Journal of Geophysical Research: Atmospheres* 2015;120:4169-4195.
- Stewart DJ, Almbrook SH, Lockhart JP, Mohamed OM, Nutt DR, Pfrang C, Marston G: The kinetics of the gas-phase reactions of selected monoterpenes and cyclo-alkenes with ozone and the NO<sub>3</sub> radical. *Atmospheric Environment* 2013;70:227-235.
- Stocker TF, Qin D, Plattner G-K, Tignor M, Allen SK, Boschung J, Nauels A, Xia Y, Bex V, Midgley PM: IPCC, 2013: Climate Change 2013: The Physical Science Basis. Contribution of Working Group I to the Fifth Assessment Report of the Intergovernmental Panel on Climate Change Cambridge University Press 2013.
- Stone D, Whalley LK, Heard DE: Tropospheric OH and HO<sub>2</sub> radicals: field measurements and model comparisons. *Chem Soc Rev* 2012;41:6348-6404.
- Tkacik DS, Lambe AT, Jathar S, Li X, Presto AA, Zhao Y, Blake D, Meinardi S, Jayne JT, Croteau PL, Robinson AL: Secondary Organic Aerosol Formation from in-Use Motor Vehicle Emissions Using a Potential Aerosol Mass Reactor. *Environmental Science & Technology* 2014;48:11235-11242.
- Vaden TD, Imre D, Beranek J, Shrivastava M, Zelenyuk A: Evaporation kinetics and phase of laboratory and ambient secondary organic aerosol. *Proc Natl Acad Sci U S A* 2011;108:2190-2195.
- Vehkamäki H, Riipinen I: Thermodynamics and kinetics of atmospheric aerosol particle formation and growth. *Chem Soc Rev* 2012;41:5160-5173.
- Vereecken L, Francisco JS: Theoretical studies of atmospheric reaction mechanisms in the troposphere. *Chem Soc Rev* 2012;41:6259-6293.
- Vereecken L, Harder H, Novelli A: The reaction of Criegee intermediates with NO, RO<sub>2</sub>, and SO<sub>2</sub>, and their fate in the atmosphere. *Phys Chem Chem Phys* 2012;14:14682-14695.
- Winterhalter R, Neeb P, Grossmann D, Koloff A, Horie O, Moortgat G: Products and Mechanism of the Gas Phase Reaction of Ozone with  $\beta$ -Pinene. *Journal of Atmospheric Chemistry* 2000;35:165-197.
- Virtanen A, Joutsensaari J, Koop T, Kannosto J, Yli-Pirila P, Leskinen J, Makela JM, Holopainen JK, Poschl U, Kulmala M, Worsnop DR, Laaksonen A: An amorphous solid state of biogenic secondary organic aerosol particles. *Nature* 2010;467:824-827.
- Zhang D, Zhang R: Ozonolysis of alpha-pinene and beta-pinene: kinetics and mechanism. *J Chem Phys* 2005;122:114308.
- Zhang X, Lambe AT, Upshur MA, Brooks WA, Gray Be A, Thomson RJ, Geiger FM, Surratt JD, Zhang Z, Gold A, Graf S, Cubison MJ, Groessl M, Jayne JT, Worsnop DR, Canagaratna MR: Highly Oxygenated Multifunctional Compounds in alpha-Pinene Secondary Organic Aerosol. *Environ Sci Technol* 2017;51:5932-5940.
- Zhang X, McVay RC, Huang DD, Dalleska NF, Aumont B, Flagan RC, Seinfeld JH: Formation and evolution of molecular products in alpha-pinene secondary organic aerosol. *Proc Natl Acad Sci U S A* 2015;112:14168-14173.